BRNO UNIVERSITY OF TECHNOLOGY
VYSOKÉ UČENÍ TECHNICKÉ V BRNĚ

FACULTY OF INFORMATION TECHNOLOGY
FAKULTA INFORMAČNÍCH TECHNOLOGIÍ

DEPARTMENT OF COMPUTER SYSTEMS
ÚSTAV POČÍTAČOVÝCH SYSTÉMŮ

DETECTION OF ANXIETY FROM BRAIN ELECTROENCEPHALOGRAM (EEG) SIGNALS

DETEKCE ÚZKOSTI ZE SIGNÁLŮ ELEKTROENCEFALOGRAMU MOZKU (EEG)

MASTER'S THESIS
DIPLOMOVÁ PRÁCE

AUTHOR **Bc. JÚLIUS MARKO**
AUTOR PRÁCE

SUPERVISOR **doc. AAMIR SAEED MALIK, Ph.D.**
VEDOUCÍ PRÁCE

BRNO 2023

BRNO UNIVERSITY OF TECHNOLOGY
FACULTY OF INFORMATION TECHNOLOGY

Master's Thesis Assignment

141163

Institut:	Department of Computer Systems (UPSY)
Student:	**Marko Július, Bc.**
Programme:	Information Technology and Artificial Intelligence
Specialization:	Bioinformatics and Biocomputing
Title:	**Detection of Anxiety from Brain Electroencephalogram (EEG) Signals**
Category:	Biocomputing
Academic year:	2022/23

Assignment:

1. Study and learn about the anxiety and how it affects the brain in terms of brain signals and images.
2. Get acquainted with signal & image processing methods as well as machine learning techniques and their application to the brain EEG signals and images.
3. Find out the challenges in detection of anxiety from brain signals and images as well as the limitations of the existing methods.
4. Design an algorithm for detection of anxiety from brain EEG signals and images.
5. Implement the designed algorithm.
6. Create a set of benchmark tasks to evaluate the quality of detection of anxiety as well as the corresponding computational performance and memory usage.
7. Conduct critical analysis and discuss the achieved results and their contribution.

Literature:

- According to supervisor's advice.

Requirements for the semestral defence:

- Items 1 to 4 of the assignment.

Detailed formal requirements can be found at https://www.fit.vut.cz/study/theses/

Supervisor:	**Malik Aamir Saeed, doc., Ph.D.**
Head of Department:	Sekanina Lukáš, prof. Ing., Ph.D.
Beginning of work:	1.11.2022
Submission deadline:	24.5.2023
Approval date:	31.10.2022

Abstract

Anxiety affects human abilities, behavior, productivity, and quality of life. Anxiety keeps us safe as part of a system that helps to control and avert danger. However, this safety system can go wrong. When such impairment emerges, it can lead to depression and even suicide. This work aims to develop a novel method of anxiety detection from brain signals, in particular electroencephalography (EEG), a non-invasive and cost-effective screening method. The proposed method incorporates microstates, which were not previously utilized for anxiety detection. Additional features in the time and frequency domain are extracted. Finally, a machine learning classifier is trained and evaluated on these features, outperforming other existing methods.

Abstrakt

Úzkosť ovplyvňuje ľudské schopnosti, správanie, produktivitu a kvalitu života. Úzkosť nás udržuje v bezpečí ako súčasť systému, ktorý pomáha kontrolovať a odvracať nebezpečenstvo. Tento systém sa však môže narušiť. Keď takéto narušenie nastane, môže to viesť k depresii a dokonca k samovražde. Cieľom tejto práce je vyvinúť novú metódu detekcie úzkosti zo signálov mozgu, konkrétne elektroencefalogramu (EEG), neinvazívnej a nákladovo efektívnej skríningovej metódy. Navrhovaná metóda zahŕňa mikrostavy, ktoré zatiaľ neboli na základe dostupnej literatúry použité na detekciu úzkosti. Extrahované sú aj ďalšie vlastnosti v časovej a frekvenčnej doméne. Nakoniec bol na týchto vlastnostiach natrénovaný a vyhodnotený klasifikátor strojového učenia, ktorý prekonal aktuálne dostupné metódy.

Keywords

anxiety, anxiety disorder, electroencephalogram, EEG, brain, microstates, machine learning

Klíčová slova

úzkosť, úzkostná porucha, elektroencefalografia, EEG, mozog, mikrostavy, strojové učenie

Reference

MARKO, Július. *Detection of Anxiety from Brain Electroencephalogram (EEG) Signals.* Brno, 2023. Master's thesis. Brno University of Technology, Faculty of Information Technology. Supervisor doc. Aamir Saeed Malik, Ph.D.

Detection of Anxiety from Brain Electroencephalogram (EEG) Signals

Declaration

I hereby declare that this Master's thesis was prepared as an original work by the author under the supervision of Mr. Malik. I have listed all the literary sources, publications and other sources, which were used during the preparation of this thesis.

.....
Július Marko
May 23, 2023

Acknowledgements

I acknowledge and appreciate the professional guidance and expertise provided by my supervisor, Mr. Malik, during the creative process of writing this thesis.

Contents

Chapter 1

Introduction

Anxiety is an emotion people experience in their lives quite often. It is characterized by an unpleasant state of inner turmoil and feelings of dread over anticipated events. Anxiety keeps us safe as part of the system that helps control and avert danger. However, this safety system can go wrong. Such impairment can lead to an anxiety disorder characterized by excessive and uncontrollable feelings of anxiety and fear without presence of an external threat. Anxiety disorders are diagnosed using various questionnaires, which are subjective methods. Therefore, there is a need for objective methods based on data to eliminate inaccurate diagnoses resulting in inappropriate treatment.

This chapter is to provide an introduction to the brain, anxiety, and brain imaging techniques. At the beginning, the brain, its anatomy, and the limbic system is discussed. The following section then focuses on the underlying mechanisms of anxiety, including current medical diagnostics methods. Finally, the chapter ends by outlining different screening methods, with emphasis on electroencephalography.

1.1 Brain

The brain is a central organ of the nervous system. It controls most of the activities of the human body, such as processing, integrating, and coordinating information it receives from the sense organs and making decisions as to the instructions sent to the rest of the body.

1.1.1 Anatomy

The primary building block of the brain is a neuron. The neuron is a type of cell that communicates with other cells. The neuron consists of a soma (neuron body), dendrites, and an axon. The soma contains a nucleus. The dendrites are cellular extensions branching out of the soma, and their function is to receive messages from other neurons. The axon is connected to the soma and carries nerve signals away to other neurons. At the end of the axon, there is an axon terminal that contains synapses. Synapses are structures that permit the passing of electric signals to another neuron. Nerve impulse, also known as an action potential, occurs when the membrane potential of a neuron rapidly increases and falls; often said to “fire”.

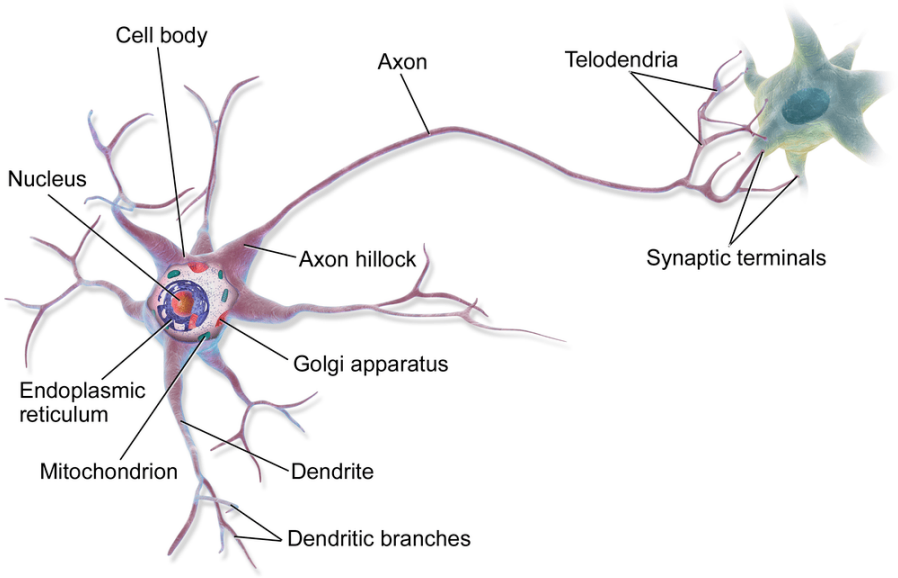

Figure 1.1: Anatomy of a multipolar neuron. Figure taken from [13].

The brain consists of about 90 billion of neurons. Neurons are interconnected and form structures. The brain is divided into the hindbrain (rhombencephalon), midbrain (mesencephalon), and forebrain (prosencephalon) [46]. The hindbrain is subdivided into the medulla oblongata, pons, and cerebellum. Medulla oblongata, pons, and midbrain are collectively referred to as the brainstem. The forebrain is subdivided into the diencephalon and the telencephalon. Diencephalon equates primarily to the thalamus and hypothalamus. The telencephalon is mainly composed of the cerebrum (cerebral cortex), the brain's largest part. The main functions of the cerebrum are sensory processing, olfaction, language and communication, learning, and memory. The cerebrum is formed by the right and left cerebral hemispheres separated by the longitudinal fissure. The corpus callosum, a large bundle of nerve fibers, links these two hemispheres. Each cerebral hemisphere is divided into six lobes: frontal, parietal, occipital, temporal, insular, and limbic lobes [46]. Limbic lobes are particularly interesting in regard to anxiety as they relate to emotional activity.

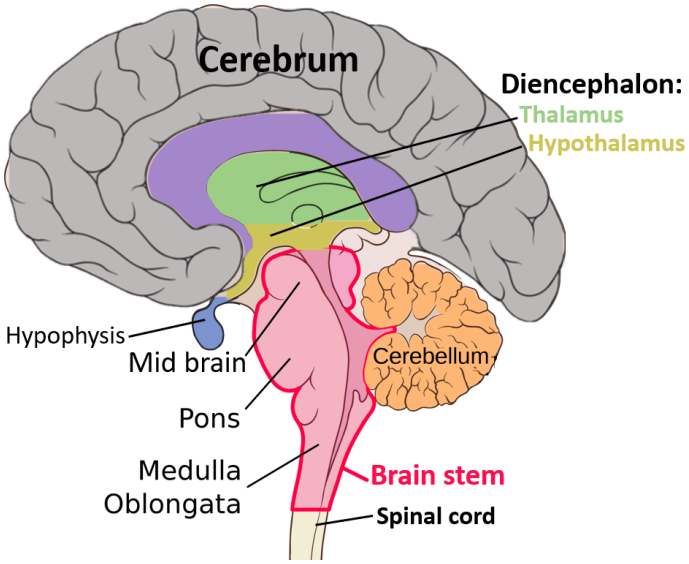

Figure 1.2: Fundamental structures of the brain. Figure taken from [38].

1.1.2 Limbic System

The limbic system is concerned with emotional and motivational activity and other essential psychological functions such as memory and learning. Most descriptions of the limbic system include the structures within the limbic lobe – the amygdaloid nuclear complex; various nuclei of the hypothalamus, the septal nuclei; nucleus accumbens; cingulate cortex; major areas of the prefrontal cortex habenula; anterior thalamic nuclei; parts of the basal ganglia; ventral tegmental area; and limbic midbrain areas, including the periaqueductal grey. The term "limbic brain" encompasses all of these structures and their projections to the forebrain, midbrain, lower brainstem, and spinal cord limbic systems [46].

When it comes to function, the thalamus is like a relay station of the brain – most of the incoming external sensory information makes a stop in here en route to the cortex. The hypothalamus is located below the thalamus and links the nervous and endocrine systems together. It regulates many of the body's essential functions, e.g., body temperature, hunger, thirst, sleep, or circadian rhythms. Every single nucleus in the limbic system tries to stimulate the hypothalamus to reach its goal depending on the situation.

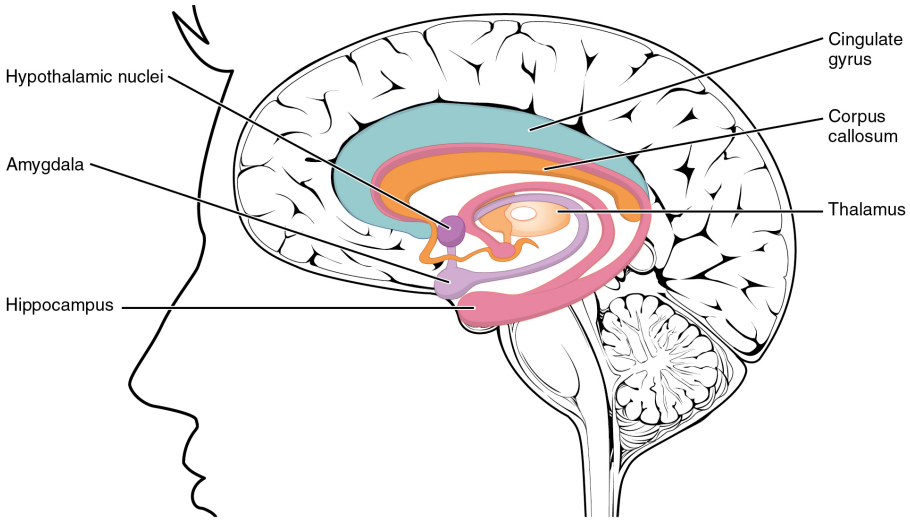

Figure 1.3: Limbic lobe with corresponding structures. Figure taken from [11].

Brain structures described in this section are involved in forming anxiety. The next section provides an overview of underlying mechanisms.

1.2 Anxiety

Anxiety is an emotion people experience in their lives quite often. It is characterized by an unpleasant state of inner turmoil and feelings of dread over anticipated events. However, anxiety keeps us safe as part of the system that helps control and avert danger. According to British psychologist Eysenck, brave individuals have died, and the anxious ones survived the Stone Age [26].

1.2.1 Mechanism

The limbic system, especially the amygdala, forms the emotion of anxiety. Anxiety is the result of the interaction between the nuclei in the brainstem (noradrenergic locus coeruleus, serotonergic nuclei raphe, and glutamatergic nucleus gigantocellularis), limbic system (especially thalamus, amygdala, and hippocampus) and the prefrontal cortex [26]. The amygdala forms the emotion of anxiety by associating sensory information from the thalamus. When the amygdala evaluates a situation as threatening, it triggers a cascade of reactions. Amygdala activates specific nucleus in the brainstem responsible for arousal and attention and activates the sympathetic nervous system, which stimulates the body's "fight or flight" response. Amygdala also increases the release of corticotropin-releasing hormone (CRH) from the hypothalamus.

These interactions lead to the activation of the stress axis: sympatho-adrenomedullary axis and the hypothalamic-pituitary-adrenal (HPA) axis. Sympatho-adrenomedullary axis responds quickly – within a few seconds. The adrenal gland (in particular, the adrenal medulla) washes out adrenaline and noradrenaline. These hormones increase heart rate, cardiac output, and blood pressure. The body needs to react fast to resolve the possibly threatening situation. Hypothalamic-pituitary-adrenal axis responds slowly – within dozens of minutes. The pituitary gland (in particular, the anterior pituitary) washes out adrenocorticotropic hormone (ACTH), which causes the increased output of cortisol from

the adrenal gland (in particular, the adrenal cortex). Cortisol is a hormone that affects several aspects of the body and mainly helps regulate the body's response to stress. The prefrontal cortex intensifies or suppresses an emotional reaction based on the experience. At any time during this series of interactions, the anxiety is over if the brain works out that the threat is no longer present.

This section described underlying mechanisms of anxiety. Anxiety happens to be formed in the deep brain areas. This might indicate that the proper diagnostics is rather difficult. Next section outlines current diagnostic methods of anxiety in medical practice.

1.2.2 Diagnostics

The problem with diagnostics of anxiety, and mental disorders in general, is that there are not enough objective methods looking directly at the brain. Mental disorders are classified by the two most widely used systems – DSM-5 (US) and ICD-10 (UK). These classification standards contain signs and symptoms that help psychiatrists categorize the illness. Diagnosing anxiety as a disorder is done by assessing the patient's thoughts and excluding other somatic disorders. In many other areas of medicine, diagnosis is set by doing a comprehensive assessment based on an objective examination of the physical state of the patient's body (e.g., assessing the risk of diabetes is done by measuring glucose blood levels). There is a need for more objective methods of indicating the state of anxiety. Brain can be inspected by various methods described in the next section.

1.3 Screening Methods

As of today, various techniques inspect the brain. The most well-established methods used for anatomical imaging are computed tomography (CT) and magnetic resonance imaging (MRI). For functional analysis, it is functional MRI (fMRI), magnetoencephalography (MEG), positron emission tomography (PET), and electroencephalography (EEG). They are usually used at a hospital and require a skilled professional, except EEG, which is relatively inexpensive, small, and easy to use.

In CT scanning, X-rays (ionizing radiation) pass through the body. In PET, a radioactive isotope is injected into the bloodstream. The amount of radiation in these methods is at a possible minimum. However, there is still some amount, so people should only be exposed to radiation when the situation needs it. It is always up to a medician to decide if the benefits overcome the risks. On the other hand, MRI/fMRI is a risk-free method, considered safe – radio waves and a magnetic field are used to produce detailed images of body tissues. Unfortunately, the main disadvantages of MRI/fMRI are the time needed to do a scan (up to an hour), cost, and the assistance of a skilled professional. Another method based on the magnetic field's principles is MEG. It measures magnetic fields produced by the brain's electrical currents. MEG provides good both temporal and spatial resolution. Unfortunately, it has similar disadvantages as MRI, mainly the device's size and cost, and requires a skilled person.

Figure 1.4: MRI machine. Figure taken from [16].

The method which appears as a trade-off between the advantages and disadvantages of the former methods is electroencephalography (EEG). Next section describes EEG in more detail.

1.3.1 Electroencephalography

Electroencephalography (EEG) is a non-invasive screening method to record the brain's electrical activity. EEG is painless and risk-free. Although it has a high temporal resolution (milliseconds), spatial resolution is limited, and thus hard to locate the exact source of the signal. The electric signal is presented as waves of varying frequency, amplitude, and shape. EEG can measure spontaneous brain activity or brain activity during an event, known as event-related potential (ERP). EEG does not record the signal of single neurons, but rather a large bundle of neurons [29]. To be precise, EEG measures postsynaptic potentials [12]. The postsynaptic potential is a potential in the dendrites of a neuron that is receiving synapses from other neurons [11].

EEG electrodes are placed on the scalp, as shown in figure 1.5. The arrangement of electrodes is standardized. For example, one widely used arrangement is the so-called 10/20 system, shown in figure 1.6. The "10" and "20" refer to the actual distances between adjacent electrodes and are either 10% or 20% of the total front–back or right–left distance of the skull. The placement of the electrodes is referred to as montage [29]. In the bipolar montage, each waveform represents the difference between adjacent electrodes. In the referential montage, one electrode is a reference, and the waveform of every other electrode is represented as the difference between the electrode and the referential electrode.

Recorded EEG signals can incorporate noise – artifacts. The artifact is an EEG signal originating from non-cerebral origins [29]. Artifacts can be introduced by internal brain function (e.g., eye-blinking) or external environment (e.g., recording in the presence of a thunderstorm). Such artifacts can usually be removed by pre-processing phase of signal processing.

Figure 1.5: Besdata Medical EEG Headset [10].

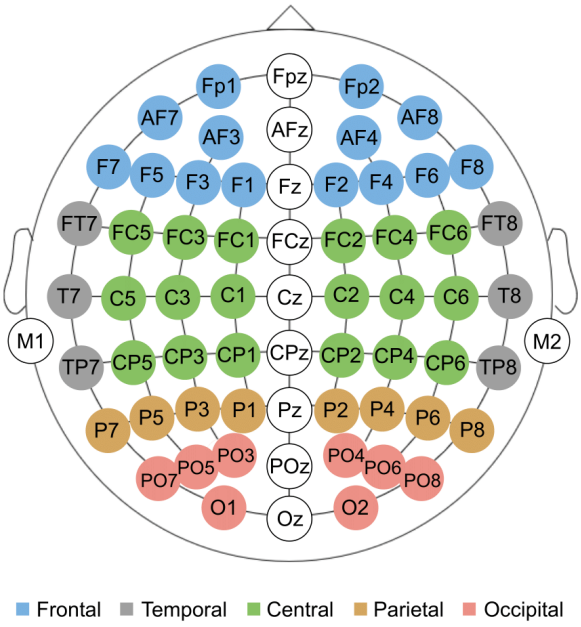

Figure 1.6: Arrangement of electrodes in 10/20 system. Figure taken from [21].

As mentioned earlier, signal that EEG records originate from large bundles of neurons. "Neurons can generate action potentials or spikes in a rhythmic pattern" [29]. These rhythmic patterns can be divided into five major categories, namely delta (δ), theta (θ), alpha (α), beta (β), and gamma (γ), shown in fig. 1.7.

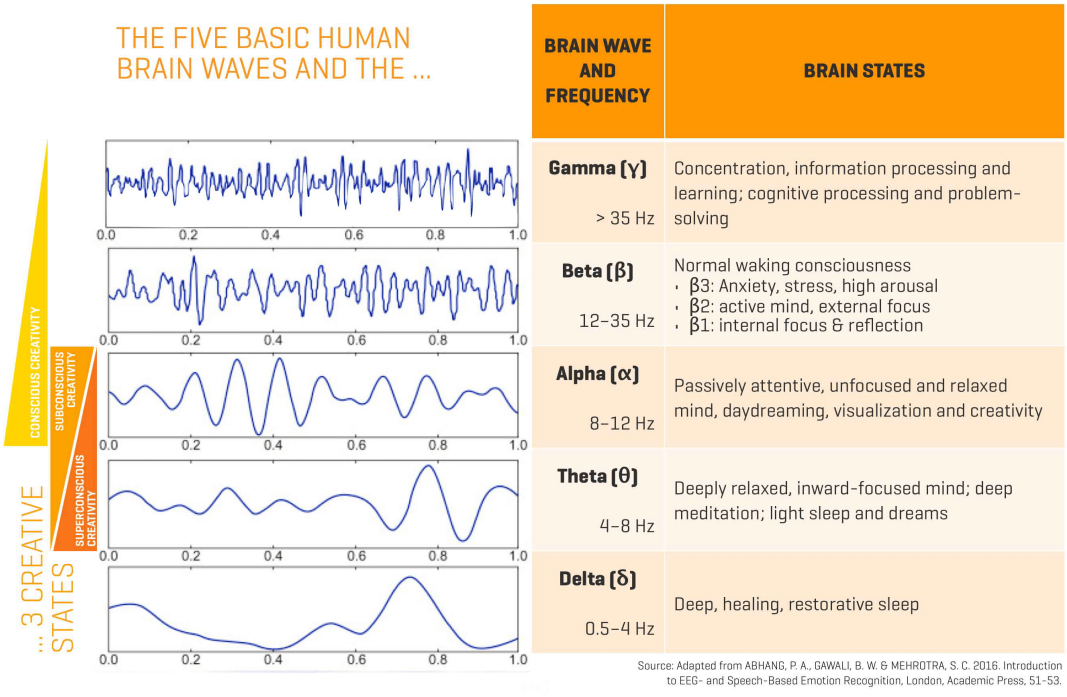

Figure 1.7: The five basic human brain waves.

Nowadays, some EEG headsets are getting easily accessible and come at a low price. The facts might support the idea of getting easier access to diagnostics of various brain abnormalities, becoming pathologic and irreversible.

1.4 Summary

This chapter focused on the biology of anxiety and its underlying mechanism. Next, screening methods were discussed, with emphasis on EEG. There is ongoing research in anxiety detection. The next chapter reviews the literature, in particular, the methods that have been proposed for anxiety detection from EEG data.

Chapter 2

Literature review

This chapter reviews existing methods of anxiety detection from EEG signals. First, methods found in the literature are described briefly, giving an overview of the essential parts of solving such task. Next, methods that are already used or have the potential to be examined in terms of anxiety detection are described in more detail. After that, existing datasets are explored. Finally, the chapter ends with a discussion of the current state based on the literature review.

2.1 Assessment Methods of Anxiety

Various methods of detecting state and trait anxiety exists in the literature – to give an overview, various studies are summarized in the next few paragraphs.

In the first study [8], authors focused on state anxiety. EEG signals of 23 healthy participants, not suffering from psychological diseases, were recorded during anxiety elicitation. Dataset consists of 13 women and 10 men with average age of 30 years old. For more information about dataset, see DASPS. Anxiety was elicited by means of face-to-face psychological stimuli, where psychotherapist helps subjects to imagine a situation that can cause anxiety. EGGs of 15s are kept, consisting of recording during self recall by subject. EEG signals were recorded using wireless Emotiv Epoc EEG headset (14 electrodes). Data were labelled using a HAM-A (Hamilton Anxiety Rating Scale) and SAM (Self Assessment Manikin). Various features were tested separately. Highest classification accuracy of 81.40% was obtained by k-NN classifier and feature Root Mean Square derived from a wavelet decomposition, in a two class classification based on SAM labelling (normal-to-light and moderate-to-severe classes). Consequently, authors produced newer paper [7], where in addition to prediction based on SAM, also examined prediction based on HAM-A, improving on lower accuracies reached in four-class classification – accuracy of 86.70% was obtained using Stack Sparse Autoencoder with large feature vector, consisting of 277 features. Authors also comment on the lower accuracy when using features from longer segments, such as 15s or 5s, stating that anxiety is evoked in shorter time, thus considering 15s and 5s trial too long as it might contain more than one emotion.

In the newer study [37], the same dataset consisting of EEG recordings of 23 healthy participants is used. The data were segmented into 1 second chunks, resulting in 4140 data instances. At first, authors performed channel selection to select statistically significant channels, which results in using only AF3, AF4, FC5, FC6, P7 and P8 channels. They also selected only subset of bands, particularly theta and beta bands. Features from these

bands were selected by applying wrapper method. Features used for classification are Rational asymmetry, Mean power, and Asymmetry Index. Various models were tested: DT, k-NN, SVM, MLP, and RF. Highest accuracy of 94.90% and 92.74% is reached using Random Forest in two-class and four-class classification respectively. Authors also mention, that classification performance is validated using leave-one-out cross-validation mechanism, where training and testing samples do not belong to the same subjects. Feature vector length is 9 and 10 for two-class and four-class respectively. These results significantly outperforms models in the former study, while still preserving small size of the feature vector.

In another study [15], authors also focused on state anxiety. EEG recordings of 34 participants during resting and meditation state. Participants were divided into non-anxiety and anxiety group, where anxiety group consisted of patients with anxiety disorder. Final labelling resulted into three classes – healthy (no anxiety), moderate anxiety and severe anxiety. Healthy class consists of recordings of healthy patients. Moderate consists of recordings of anxious patients during meditation; and severe consists of recordings of anxious patients after meditation. Power spectrum density was used as a feature. This feature was used for classification by SVM, resulting in accuracy of 92.48%.

In a study using low density headset [5], authors focused on trait anxiety. EEG signals of 65 participants were recorded during resting state. Information about medical conditions of participants is not specified. The age of the participants ranges from 18 to 40 years. Wireless MUSE EEG headband was used (4 electrodes). Unfortunately, dataset is not available on the link provided in the paper. Data were labeled according to STAI (Y2), which is the standard questionnaire designed for measurement of state and trait anxiety. In two class labelling, 35 are labelled as non-anxious participants and 30 as anxious participants. In three class labelling, 27 participants are labelled as non-anxious, 17 as low-anxious and 21 as highly anxious. After the recording, data were preprocessed and used for classification. TP9 and AF8 were found to be significantly different channels and thus used for classification. Features obtained after feature selection are signal peak-to-peak value and signal energy. Models that were used are Multilayer perceptron, Logistic regression and Random forest. The results were calculated using 10-fold cross-validation scheme. Highest accuracy of 87.69% was obtained using Random Forest classifier, discriminating between non-anxious and anxious subjects. Classification into three classes (non-anxious, low-anxious and highly anxious) resulted in lower accuracy of 83.07%. Feature vector length were 2 and 3 for two-class and three-class detection respectively, which is surprisingly low. Also, extracted features are very simple.

Study related to severity assessment of social anxiety disorder (SAD) using deep learning models on brain effectivity connectivity focused on trait anxiety [3]. EEG signals of 88 participants were recording during resting state. Participants were recruited from 502 respondents. No link to dataset is provided. Dataset contains balanced distribution of classes, in particular of 22 healthy group, 22 having mild SAD, 22 having moderate SAD, and 22 with severe SAD. This grouping into different classes was based on self-assessment of the SIAS (Social Interaction Anxiety Scale). All participants were healthy mentally and physically, with no history of psychiatric disabilities. Data were collected using shielded ANT Neuro cap (32 electrodes). Feature used is effective connectivity of the DMN (Default mode network), particularly PDC (Partial directed coherence) matrices of size 8x8 are obtained for each frequency band (one matrice carry information from signal duration of 3s). These are fed into CNN, LSTM and CNN + LSTM. The highest accuracy of 93 % was obtained using CNN + LSTM. However, no information about validation technique

used are available. Authors then compared their method to the former CNN or LSTM methods found in the literature, where their method reached highest performance. Except high classification accuracy, authors also located cortical sources of activity using effective connectivity features, and were able to demonstrate the differences in the brain activity between healthy and SAD participants, during resting state.

In the next sections, methods that are already used in studies described above, or have the potential to be examined are described in more detail.

2.1.1 Event-Related Potential

An event-related potential (ERP) is the measured brain response to a specific event. It provides a direct, instaneous, millisecond-resolution measure of neurotransmission-mediated neural activity [32]. ERPs waveforms are described according to latency and amplitude. Amplitude can be positive (P) or negative (N). For example, N170 is known ERP component that relates to visual object recognition of faces, objects, and words [43]. In this component, "N" stands for negative amplitude, and "170" determines the amplitude's peak time in milliseconds from onset of stimulus.

ERP components are extracted from recorded EEG signal. First, EEG signal is amplified and artifacts are removed. Then, ERPs are isolated from the EEG signal by averaging procedure. This is done by marking the events that happened at specific times, such as the onset of each stimulus. Then, these marks are used as a time-locking point to extract segments of the EEG surrounding each event. There is need to perform many trials to extract the activity related to stimulus processing from unrelated activity. Using averaging procedure, related activity is kept, and unrelated activity discarded. This is because related activity has to be similar in all trials, while unrelated activity can be seen as varying between the trials. Therefore, unrelated activity has to cancel out itself after applying averaging procedure. However, different ERP components require different number of trials. For large components, such as P300, 10-50 trials per subject are enough, while for smaller components like P100, 100-500 trials are needed [32].

ERPs are studied in terms of anxiety. Next subsection focuses on findings from systematic review on attentional control in anxiety disorders, suggesting error-related negativity as a promising marker of clinical anxiety [34].

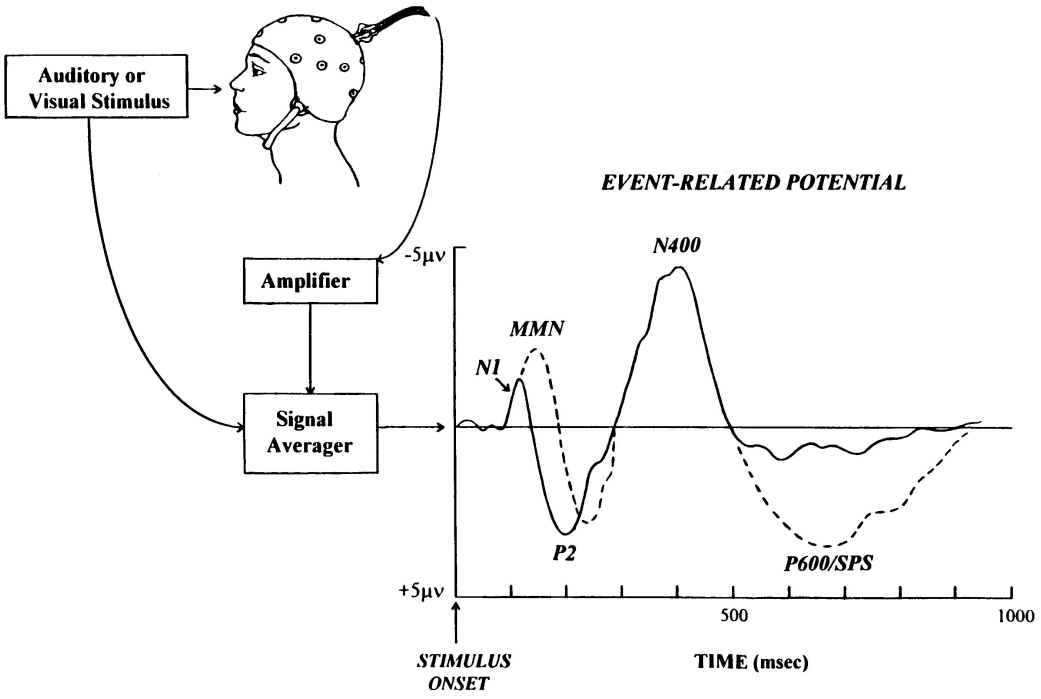

Figure 2.1: Event-related potential (ERP). Figure taken from [28].

Error-Related Negativity (ERN)

The error-related negativity (ERN) seems promising as a robust, transdiagnostic trait marker of clinical anxiety. These findings originate from the systematic review of error-related negativity and correct-response negativity [34]. ERN is a type of event-related potential reflecting a response-locked negative deflection which occurs when a behavioural error is made. ERN component peaks around 80–110 ms after error is made [33].

A total of 56 of the 66 studies measuring ERN found significantly greater ERN amplitudes were associated with clinical anxiety. Review also aimed to assess correct-response negativity (CRN), but only 20% of reviewed studies found significant changes in amplitude. While the review suggests the ERN as a trait marker of clinical anxiety, they limit this interpretation by past findings that the ERN is sensitive to state-specific manipulations, including e.g., monetary incentive or caffeine; that the ERN is also related to other cognitive processes such as working memory, and is also related to other psychological disorders not related to anxiety. The review is also limited by the fact that only 6 of all studies used emotional attentional control tasks, making it difficult to draw firm conclusions on the effects of emotion on attentional control and if there are differences between emotional and non-emotional attentional control. Another limitation is the gap in the literature on older adults (60+), given that past research has shown a potential age-related decline in attentional control. No studies have investigated the ERN's sensitivity, specificity, or incremental validity to make anxiety disorder diagnoses, so the paper's authors are not going as far as describing the ERN as a diagnostic marker of anxiety disorders. However, they consider ERN as one of the elements in an array of objective biological markers of anxiety disorders.

Despite its limitations, all studies showed a consistent pattern of an increase in ERN amplitude, which suggests that the ERN has the potential to be used as a trait marker of clinical anxiety.

2.1.2 Source Localization

Source localization is a major problem in EEG. Localizing sources of the brain activity helps to understand various functional abnormalities and cognitive behaviour of the brain and leads for the specification for diagnoses of various brain disorders. The localization process involves the prediction of scalp potentials from the current sources in the brain (forward problem) and the estimation of the location of the sources from scalp potential measurements (inverse problem) [29]. Forward problem is easy – scalp potentials are measured by scalp electrodes placed on the skull. However, inverse problem suggests predicting the actual sources of brain activity from measured scalp potentials. The problem is that inverse problem has non-unique solutions, which means many models can fit the data. Additionally, the estimated data are tainted with errors, so estimated model always differ from true model, therefore predicted model is just an approximation of the true model. Based on these properties, the inverse problem is said to be ill posed problem.

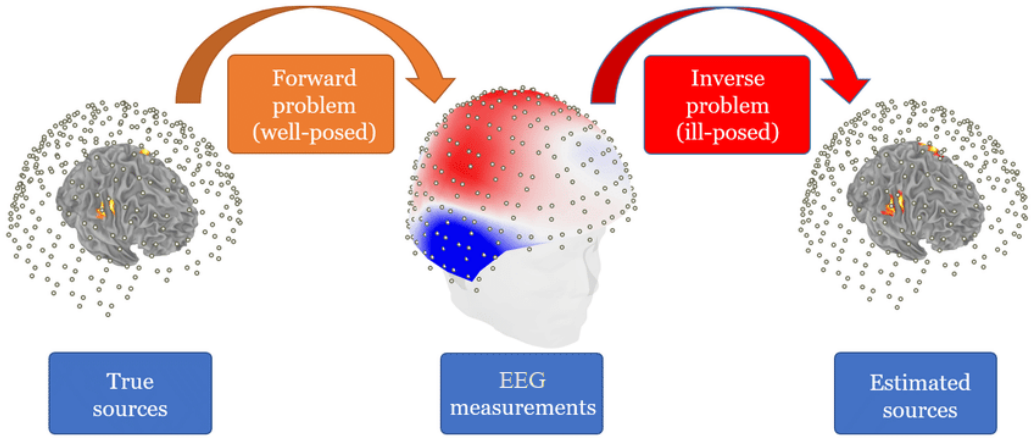

Figure 2.2: Forward and inverse problem. Figure modified, taken from [39].

Minimum norm imaging (MNI) was used to exclude non-active cerebral areas from further statistical EC analysis [3]. Authors computed source localization for the 32-electrode EEG, applying MNI in Brainstorm [49], which is documented and freely available for download online under the GNU general public license.

2.1.3 Time Series Analysis

Hjorth Parameters

Hjorth parameters were used in many former EEG studies [8]. Hjorth parameters are measurement of basic signal properties by means of a time-base calculation. They consists of three parameters – activity, mobility, and complexity [24].

Activity is measure of the squared standard deviation of the amplitude, sometimes referred to as the variance or mean power:

$$A = var(y(t)) \tag{2.1}$$

Mobility is a measure of the standard deviation of the slope with reference to the standard deviation of the amplitude. It is expressed as a ratio per time unit and may be conceived also as a mean frequency:

$$M = \sqrt{\frac{var(\frac{\mathrm{d}y(t)}{\mathrm{d}t})}{var(y(t))}} \tag{2.2}$$

Complexity is expressed as the number of standard slopes actually generated during the average time required for generation of one standard amplitude as given by the mobility. Due to the non-linear calculation of standard deviation this parameter will quantify any deviation from the sine shape as an increase from unity:

$$C = \frac{M(\frac{\mathrm{d}y(t)}{\mathrm{d}t})}{M(y(t))} \tag{2.3}$$

In research related to anxiety detection and it's severity, Hjorth parameters were calculated for all EEG channels [8]. These parameters were then used as a features put into k-NN classifier, reaching accuracy of 81.40% in binary classification, discriminating between normal or light anxiety, and moderate or severe anxiety. Authors concluded that Hjorth parameters are the most simple features to extract from an EEG signal, yet they produce a significant accuracy throughout all types of datasets.

2.1.4 Frequency Analysis

Delta-Beta Coupling

Delta-beta coupling represents the cross-frequency correlation between the amplitude of delta-band and beta-band oscillations. Coupling between delta (1–4 Hz) and beta (14–30 Hz) oscillations is posited to reflect subcortico-cortical communication and stress regulation [40].

There are different types of cross-frequency coupling – phase to phase coupling, power to power coupling, frequency to frequency coupling, or combinations, resulting in six different types [27], shown in figure 2.3.

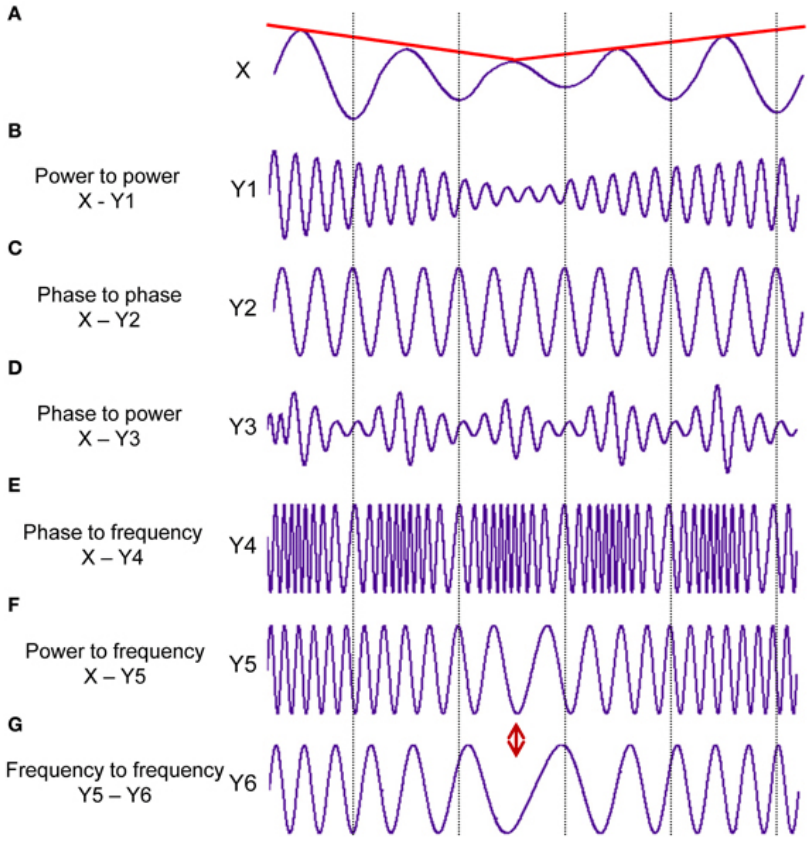

Figure 2.3: Different types of cross-frequency coupling (CFC). Signal X at a given constant frequency fluctuating in the amplitude over time (red line). Then, possible couplings are showed: (B) power to power (C) phase to phase (D) phase to power (E) phase to frequency. (F) power to frequency (G) frequency to frequency. Figure taken from [27].

In the review study of various biomarkers of social anxiety disorder [2], delta-beta cross-frequency correlation was investigated. Authors of the study consider delta-beta cross-frequency correlation as a widely used measure in the investigation of social anxiety. They reviewed literature related to delta-beta coupling in various states – resting, anticipatory, and recovery state. Resting state EEG recordings denote spontaneous neural activity [9]; anticipation state is period in which participant anticipates the fearful situation; and recovery state happens after the anticipation state. Resting state and anticipatory state are believed to be promising measure in terms of social anxiety disorder. Regarding recovery state, authors suggest doing further research to assess whether the delta-beta coupling in recovery state can serve as a measure of social anxiety disorder.

Amplitude Asymmetry

Amplitude asymmetry can be computed by comparing the EEG signal from two different electrode locations. It was calculated using alpha band power, that can be extracted using discrete wavelet transform (DWT) [8]. For more information about DWT, see Time-Frequency Analysis. To calculate the asymmetry index, the continuous signal must be broken into small parts. Scientific studies recommend overlapping epochs with each limited

to a duration of 1-2 seconds [8]. Then, the asymmetry index equals to natural logarithm of left side channels subtracted from the right ones (L-R):

$$AI = \ln(\alpha)|_{LChannel} - \ln(\alpha)|_{RChannel} \tag{2.4}$$

Various researches demonstrated that the asymmetry index is potential biomarker related to anxiety. Asymmetry index has reduced during an anxiety state in comparison to relaxed state [5]. Frontal asymmetry (the relative difference in power between two signals in different hemispheres) has been suggested as biomarker for anxiety [8]. Frontal asymmetry within the alpha band can be inversely related to stress/anxiety. However, in another review, authors found incosistent findings, thus indicating that frontal alpha asymmetry is not a trait mark of SAD, but may be related to SAD in the presence of some definite extreme stressors, suggesting more studies need to focus on the coexistence of SAD and other mental disorders [2].

Fourier Transforms

Discrete Fourier transform (DFT) is used for analyzing discrete-time finite-duration signals in the frequency domain. DFT transforms a sequence of N complex numbers:

$$\mathbf{x}_n := x_0, x_1, \ldots, x_{N-1} \tag{2.5}$$

into another sequence of complex numbers,

$$\mathbf{X}_k := X_0, X_1, ..., X_{N-1} \tag{2.6}$$

which is defined by:

$$X_k = \sum_{n=0}^{N-1} x_n . e^{-\frac{i2\pi}{N} kn} = \sum_{n=0}^{N-1} x_n . \left[cos\left(\frac{2\pi}{N}.kn\right) - i.sin\left(\frac{2\pi}{N}.kn\right)\right] \tag{2.7}$$

To obtain a fast or real-time implementation of (2.7), one often uses a fast Fourier transform (FFT) algorithm, which makes use of the symmetry properties of DFT [30]. There are many variations of FFT algorithms.

Short-time Fourier transform (STFT) is a sequence of Fourier transforms of a windowed signal. STFT provides the time-localized frequency information for situations in which frequency components of a signal vary over time, whereas the standard Fourier transform provides the frequency information averaged over the entire signal time interval [30].

Band Power

Band Power features are the most popular features in the context of EEG-based emotion recognition [8]. The decomposition of the overall power in the EEG signal into individual bands is commonly achieved through Fourier transforms, or alternatives like short-time fourier transform (STFT) or estimation of power spectral density (PSD) using Welch's method.

Peak power is the highest power in an EEG signal. Absolute Power is the power of an EEG band independent of the power of the other bands:

$$P = \sum \left| fft(x)^2 \right| \tag{2.8}$$

where x is an EEG signal and *fft* is Fast Fourier Transform.

The study related to anxiety reduction concluded that an increase in the amplitude of the beta band of the EEG signal was associated with the anxiety level of an individual [5]. Another finding from this study is that after the treatment with the use of VR, beta activity in the anterior cingulate cortex was significantly reduced. These findings might indicate that the beta band amplitude is potentially associated with anxiety.

2.1.5 Time-Frequency Analysis

Wavelet Transform

Wavelet transform offers a generalization of STFT. From a signal theory point of view, similar to DFT and STFT, wavelet transform can be viewed as the projection of a signal into a set of basis functions named wavelets. Such basis functions offer localization in the frequency domain. In contrast to STFT having equally spaced time-frequency localization, wavelet transform provides high frequency resolution at low frequencies and high time resolution at high frequencies [30].

Alpha and beta band wavelet coefficients were found to be highly correlated with the anxiety level [5]. Another study states that time-frequency features obtained after a wavelet transform achieved best rates in classification [8]. One of the features that perform very well is Root Mean Square (RMS) using DWT. The highest accuracies based only on the RMS feature were 77.40% and 73.60% for two class and four class classification respectively, discriminating between the severity of state anxiety. In two-class, between light and severe; in four-class between normal, light, moderate and severe anxiety. RMS is derived from a wavelet decomposition with the function "db5" for 5 levels and is extracted for each frequency band:

$$RMS(J) = \sqrt{\frac{\sum_{i=1}^{j} \sum_{n_i} D_i(n)^2}{\sum_{i=1}^{j} n_i}} \tag{2.9}$$

where D_i are the detail coefficients, n_i the number of D_i at the i^{th} decomposition level, and j denotes the number of levels.

Hilbert-Huang Spectrum

Hilbert-Huang spectrum (HHS) is considered as a new way to extract necessary information from EEG data, since it defines amplitude and instaneous frequency for each sample [8]. In the work, they computed HHS for each signal using the Empirical Mode Decomposition (EMD) to obtain a set of Intrinsic Mode Functions (IMFs), representing the original signal. Each IMF represents different frequency components of original signals. Extracted features are Hilbert Spectrum (HS) and instantaneous energy density (IED) level. The decomposition into IMFs resulted in 10 IMFs per each channel. However, features obtained through HHS did not lead to a great accuracy (64%), despite authors commenting that many researches proved this approach to perform well.

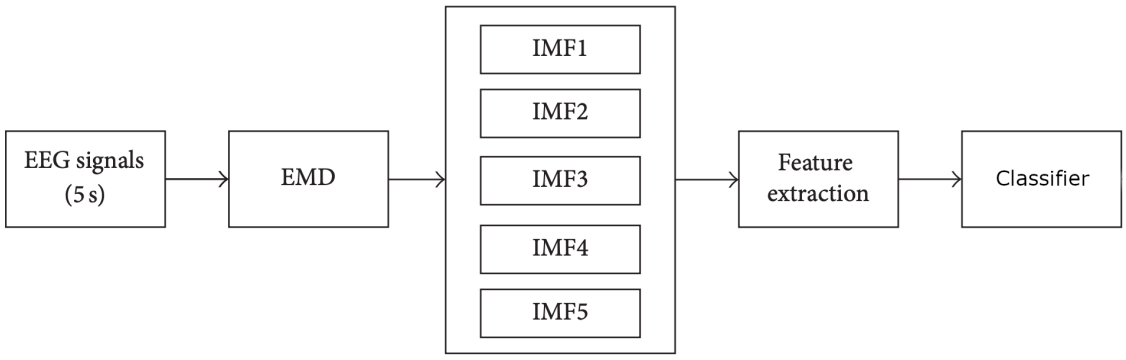

Figure 2.4: Example block diagram showing schema of extracting Hilbert-Huang spectrum. First, EEG signal is windowed into 5 second chunks. Then, EMD is used to obtain a set of IMFs. Lastly, features are extracted and used for classification. Figure taken from [53].

2.1.6 Connectivity Analysis

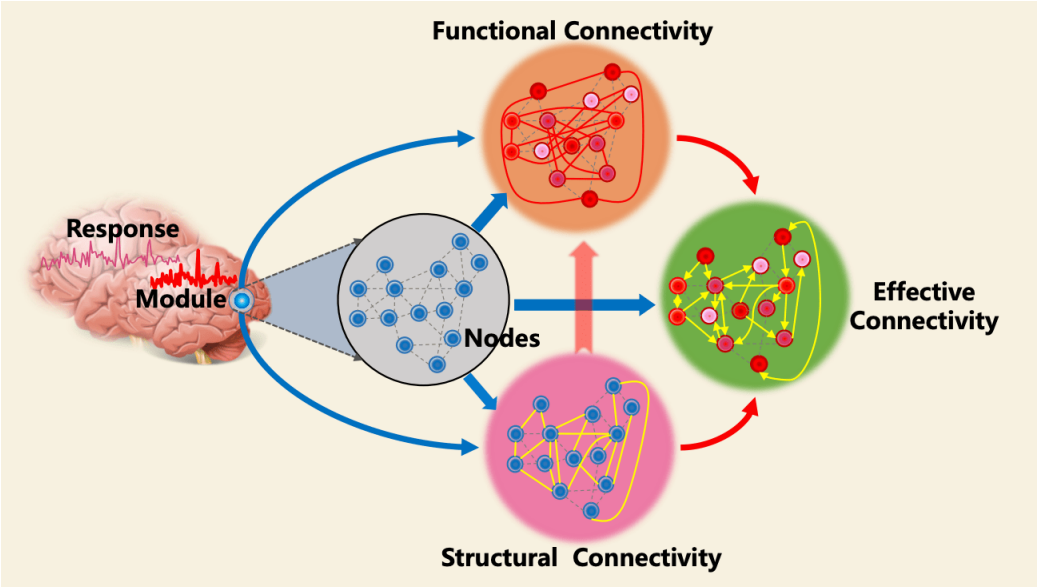

Figure 2.5: The three types of connections between brain nodes: functional connectivity, structural connectivity, and effective connectivity. Figure taken from [52].

Functional Connectivity

Functional connectivity (FC) is considered when activities within nervous system are highly correlated over time. FC refers to the statistical relationship between signals from electrodes. Structural connectivity is necessarry to assess the functional connectivity.

Phase-Lag Index

Phase-Lag index (PLI) is a functional connectivity measure to obtain reliable estimates of phase synchronization that are invariant against the presence of common sources (e.g. due to volume conduction, multiple EEG electrodes can potentially measure signal from one source) [45]. Let $\Delta\Phi(t_k)$ be the time series of phase differences, then PLI is defined as follows:

$$PLI = |\langle \text{sign}\,[\Delta\Phi(t_k)]\rangle| \tag{2.10}$$

where sign is signum function. The PLI ranges between 0 and 1, with 0 indicating no coupling due to volume conduction and 1 indicating true, lagged interaction.

PLI is commonly used to extract the adjacency matrix of functional connectivity of brain networks in five bands [51]. In one study, authors mentioned phase-lag index to use for features selection [4]. The adjacency matrix was obtained by the PLI algorithm, and then converted into a binary matrix that determined whether there was an edge, choosing an appropriate threshold, which authors set to 0.04 in this experiment. The brain network (BN) was then used as an input for the classifier. Best results were obtained using CNN model, with accuracy of 67.67%.

In a study on SAD, using the functional connectivity of the resting-state network, application of weighted PLI to EEG electrodes showed an increase in the enhanced fluctuation in oscillatory theta-rhythm coherence in the mid-frontal regions, proving that SAD has higher connectivity in the resting-state in SAD patients than in healthcheck group [2].

Instead of PLI, Prefrontal Lateralization can be used. This is a common method in evaluation of anxiety and depression patients [4]. It is defined as $ln(R) - ln(L)$, where R is the power spectral density of each band in the right brain, and L is that of the left brain. If the score is positive, the activity is stronger in the left prefrontal lobe than in the right prefrontal lobe. If the score is negative there is no left lateralization.

Authors of the review compared BN and Prefrontal lateralization, reaching to a conclusion that BNs performed better with CNN than with prefrontal lateralization [4].

Effective Connectivity

Effective connectivity (EC) is a combination of physical connections and functional connectivity because effective connectivity can effectively identify the network of causal influences of one neural unit over others within the brain [2]. Calculating EC is more challenging than determining functional brain connectivity.

EC is commonly estimated using different tools, including phase slope index (PSI) and partial directed coherence (PDC). These methods are based on Granger causality principle.

Granger Causality

The fundamental basis of estimates of causal relations using Granger Causality is the fact that a cause precedes the effect. Granger causality (GC), which identifies directed connections from time-series data, presents itself as an effective and widely used statistical method that locates natural implementation in neuroscience studies. The GC concept reveals that if a neural signal $Y(t)$ implies information in past values that assist in the prediction of neural signal $X(t)$, $Y(t)$ is believed to cause $X(t)$ [3].

There are different frequency domain Granger causality measures, such as Partial Directed Coherence (PDC) or directed transfer function (DTF).

Partial Directed Coherence

Partial directed coherence (PDI) is a technique based on the MVAR and the concept of partial coherence and Granger causality. The PDC from channel j to channel i indicates the directional flow of information from one activity site to another. PDC values are in the range of $[0, 1]$. PDC value from channel j to channel i can be expressed as follows:

$$PDC_{ij} = \frac{A_i j(\overline{f})}{\sqrt{a_j - H(f)\overline{a}_j(f)}} \tag{2.11}$$

where $\overline{a}_j$(f) $(i = 1, 2, \ldots, M)$ represents the i^{th} columns of the matrix $\overline{A}(f)$ and PDC_{ij} represents the directional influence and intensity of the information flow from channel j to channel i at a frequency of f.

In the study related to deep learning models based on effective connectivity features [3], PDC was discussed. PDC was used as an effective connectivity feature for social anxiety disorder prediction. The hyperactivity of DMN regions in higher severity of SAD indicates neural correlations associated with social anxiety disorder's (SAD) symptoms severity. Default mode network (DMN) is usually active when a person is not focused on any particular task and the brain is at wakeful rest. EEG in DMN is considered fundamental for identifying the brain dysfunction in SAD in resting state. Therefore, PDC was applied to the DMN-related regions for the estimation of the effective connections between them. The calculation of the PDC matrix for each frequency band was obtained using continuous 3-second segments of EEG, which was recorded using 32-channel shielded cap (ANT Neuro). This method reached accuracy of 93% using CNN and LSTM.

In this study, they also performed EC analysis to calculate the mean EEG activation in the brain sources. It was done by averaging PDC matrices across all epochs for each subject and then averaged within each group. There are 60 segments of 3 seconds each, per subject. This results in topographic maps of the averaged peak activity of EC and the activated areas associated with different anxiety severities and healthy group in five different frequency bands. Then, multiple cortical sources were localized, using brainstorm toolbox. Visualization of the computed EC source from EEG activity in the alpha band is shown in figure 2.6. It was proved that precuneus is the most active region in severe and moderate SAD groups compared to healthy and mild group. Healthy group also showed higher information flow in the central mPFC region compared to other groups, which indicates higher cognitive functions. Mild and moderate groups have shown greater information flow in the left mPFC than the other groups.

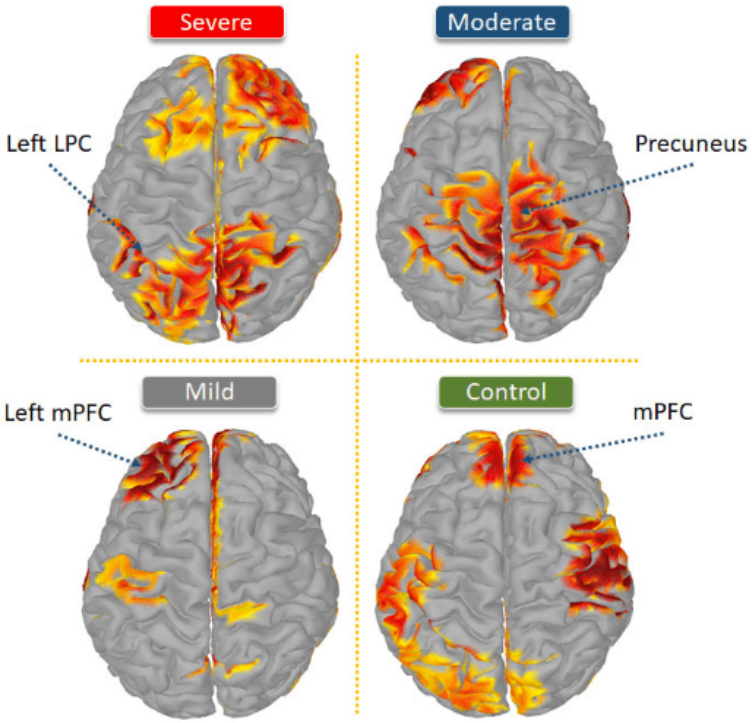

Figure 2.6: Visualization of the computed EC source from EEG activity in the alpha band. It represents the highest 30% of EC values at significant level, $p < 0.05$. Figure taken from [3].

Partial directed coherence is a powerful method to assess the effective connectivity of the brain.

2.2 Classification

This section summarizes findings from literature in terms of classification, with greater detail on models.

2.2.1 Preprocessing

Preprocessing is an important step in classification pipeline. Data needs to be preprocessed to remove unwated elements in the data.

Many researches mention the use of FIR band-pass filter. FIR band-pass filter is used to eliminate the high-frequency electrocortical artifacts, signal noise, and low-frequency deflections. For example, in one study FIR-band pass was used to acquire signal segments between the frequency range of 0.4 and 50 Hz [3].

2.2.2 Feature Selection

Feature selection is the process of selecting important features. Wrapper method, also known as sequential feature extraction is a feature selection method used to select important features. It was employed in two studies on anxiety [5, 4]. This method select subset of

features with highest classification accuracy. The algorithm starts with empty set, and then iteratively adds features, and stops when adding of feature does not improve accuracy.

2.2.3 Models

Multilayer Perceptron

Multilayer Perceptron (MLP) is a fully connected feedforward artificial neural network. It consists of three types of layers – the input layer, output layer and hidden layer. Each neurone of a layer is connected to each neurone of the next layer so that only forward transmission through the network is possible, from the input layer to the output layer through the hidden layers [25]. The training of an MLP is accomplished by using a back-propagation algorithm [44].

MLP was used in study related to EEG detection of trait anxiety using low-cost EEG headband [5]. MUSE headband with 4 channels was used. Network used has four-layer hidden network with a sigmoid activation function and a learning rate of 0.3 and 0.2 respectively. The results were calculated using a 10-fold cross-validation scheme. Training and testing data never belong to the same subject. The best results were obtained by using feature selection and channel selection, reaching accuracy of 76.92% accuracy in binary classification, discriminating between non-anxious and anxious class. Classification into three classes (non-anxious, low-anxious, high-anxious), only 56.92% accuracy was reached. MLP doesn't perform very well on this data.

Next model used in this study was Logistic regression, described in the next section.

Logistic Regression

Logistic regression is a binary classification model that can be generalized to multiclass classification [48]. It takes a linear combination of features and applies a nonlinear sigmoidal function to them [6]. Mathematically, Logistic Regression is the process of fitting the weights of the model to minimize loss on a data set [44].

Best results were obtained, again, by using feature selection and channel selection. Highest accuracy of 70.76% accuracy was reached in binary classification tasks, discriminating between non-anxious and anxious class. Classification into three classes (non-anxious, low-anxious, high-anxious), 52.30% accuracy was reached [5]. Logistic regression performed even worse than MLP.

Last model that was discussed in that paper is Random Forest.

Random Forest

Random forest (RF) is a machine learning method that works by constructing many decision trees. When used for classification, a random forest obtains a class vote from each tree, and then classifies using majority vote; whereas when used for regression, the predictions from each tree are simply averaged [22].

The number of decision trees for the RF classifier used in the study is 100 [5]. RF reached accuracy of 87.69% accuracy in binary classification, discriminating between non-anxious and anxious class. Classification into three classes (non-anxious, low-anxious, high-anxious), 83.07% accuracy was reached. Random Forest reached highest accuracy in the study, compared to Multilayer perceptron and Logistic regression.

Random Forest classifier was also discussed in the review related to machine learning methods for anxiety detection [4]. Among other ML methods, RF reached the best perfor-

mance. Three different studies mentioned in the review reached accuracy of 94.92%, 88%, and 78.60% with leave-one-out cross validation for first two, and 10-fold cross validation validation for the last. The first study tested various models – DT, kNN, SVM, MLP, and RF; with RF outperforming all of them. They've used DASPS dataset, described in section DASPS. Classification was done for two classes and four classes, discriminating between the severity of state anxiety. In two-class, between light and severe; in four-class between normal, light, moderate and severe anxiety.

K-Nearest Neighbors

K-nearest neighbors (k-NN) is a supervised machine learning method used for classification and regression. The belonging to the class is decided based on the k closest training examples in a data set.

Using k-NN, authors of one study achieved best results were obtained when the trial length is 1s, k-NN classifier using Hjorth features reaches 81.40% [8]. Authors compared different durations, resulting in a conclusion that state anxiety may be evoked in 1 second, but longer segments like 5 seconds or even 15 seconds might be too long and might contain more than one emotion. For example, using 15s segments from DASPS dataset, accuracy of only 67.07% was obtained.

Support Vector Machine

Support vectors machines (SVM) is a supervised machine learning method. SVM maps training examples to maximise the width of the gap between the two categories. New data are mapped into that same space and predicted to belong to a category based on which side of the gap they fall. SVM can be also used for multiclass classification.

In one study on state anxiety detection participants were divided into three classes – healthy (no anxiety), moderate anxiety and severe anxiety [15]. SVM obtained high accuracy of 92.48%, using power spectrum density feature.

Deep Learning

Convolutional neural network (CNN) is a type of artificial neural network that use a mathematical operation called convolution. CNN consists of convolutional layers, pooling layers and fully connected layers. Network is trained using a backgpropagation algorithm.

Long short-term memory (LSTM) is also a type of artificial neural network. Main difference between CNN is that the LSTM can have feedback connections.

Study related to deep learning models assesing severity of anxiety [3], CNN and LSTM were discussed. Authors recruited participants to create a dataset. Dataset contains EEG data of 88 participants during resting-state (3 minutes per participant). Subjects were assigned anxiety severity based on their self-assessment reports of the SIAS (Social Interaction Anxiety Scale). To ensure equal class balance, EEG recordings from 22 participants are used for each class - mild, moderate, severe and healthy group. Eight important electrodes were selected by process of MNI. Models were trained using EC features belonging to the DMN regions. PDC matrices from 5 bands were combined to be the input to the CNN and CNN + LSTM models. Combining CNN and LSTM together, model reached accuracy of 93%.

2.3 Datasets

There are various datasets used for anxiety detection that can be found in the literature. Generally, they can be divided into two groups, based on the environment in which they were recorded – either resting state EEG, where participant tries to do nothing, remains calm and minimizes movement; or during anxiety elicitation, where usually anxiety is induced in a safe environment with the help of psychotherapist.

Regarding the first group, there are two resting state EEG datasetes. First dataset comes from the study on anxiety detection from EEG headband with only 4 electrodes [5]. Signals of 65 participants were recorded, but there is no information medical conditions of participants. Second dataset is from study assessing severity of anxiety using 32 channel EEG headset [3]. EEG signals of 88 participants were recorded during resting state, where all participants were healthy (both physically and mentally).

Moving to the datasets recorded during anxiety elicitation, two datasets are found. First one contains recordings from 34 participants [52]. This is the only dataset consisting of both healthy and anxiety disorder participants. Second dataset recorded during anxiety elicitation consists of 23 healthy participants, not suffering from psychological diseases [8].

Regarding access to the datasets, only the last dataset mentioned is available publicly and free to download. Due to this fact, more studies used this dataset for their research. The dataset is named "DASPS", and is described in the next section.

2.3.1 DASPS

Dataset named DASPS was presented, consisting of EEG recordings from 23 healthy subjects (not suffering from psychological diseases) during anxiety elicitation [8]. 13 women and 10 men with an average age of 30 years old. EEG data were recorded using a wireless EEG headset, the Emotiv EPOC 14 channels and 2 mastoids placed according to the international 10-20 system.

They defined their own experimental procotol, shown in figure 2.7. In the protocol they used actual exposure to the feared stimulus. A patient is confronted with a situation in which the stimulus that provoked the original trauma is present. The trial consists of six situations. The anxiety level was calculated before stimulation according to the Hamilton Anxiety Rating Scale (HAM-A). HAM-A provides 14 items, each one contains a number of symptoms that can be rated on a scale of zero to four. Experiment starts with closed eyes and minimized gesture and speech. Psychotherapists starts by reciting the first situation and helps the subject to imagine it. This phase is divided into two stages: recitation by the psychotherapist for the first 15 sec and recall by the subject for the last 15 sec. When time is over, the subject is asked to rate how he felt during stimulation using the Self Assessment Manikin (SAM). It has two rows for rating: valence, ranging from negative to positive; and arousal, ranging from calm to excited. This trial is repeated until the sixth situation. At the end of the experiment, some items from HAM-A are re-evaluated.

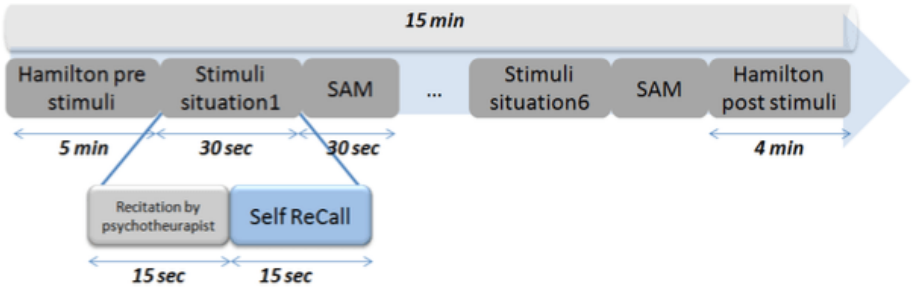

Figure 2.7: The experimental protocol of anxiety stimulation used to create DASPS dataset. Figure taken from [8].

HAM-A scores were collected both before and after the trials. Groups are assigned based on the following intervals – score in interval 0-12 is for normal anxiety, 13-19 is for light anxiety, 20-25 is for moderate anxiety, and >25 is for severe anxiety. Based on the scores before experiment, there are 4 participants with normal anxiety level, 6 light, 6 moderate, and 7 severe. Based on the scores after the experiment, there are 2 participants with normal anxiety level, 5 light, 3 moderate, and 13 severe. Based on the comparison of HAM-A before and after the trials, number of participants with severe anxiety increased from 7 to 13 denoting the impact of elicitation of participants' anxiety level. HAM-A questionnaire can be found in appendices, see A.1.

SAM scores were collected after every stimuli situation, therefore six per participant. Authors relies on the definition by Russell, who defines anxiety as: Low Valence and High Arousal. Groups are assigned based on the following intervals – valence > 5 and arousal < 5 is for normal, valence 4-5 and arousal 5-6 for light anxiety, valence 2-4 and arousal 6-7 for moderate anxiety, 0-2 Valence and 7-9 Arousal for severe anxiety. Using length of the segment equal to 15 seconds, labeling resulted into 156 normal, 20 light, 10 moderate, 90 severe segments. SAM questionnaire can be found in appendices, see A.2.

Along with the creation of dataset, authors also performed classification, using SAM scores. Highest accuracy reached was 74.60% for classification into four classes and 83.50% for two classes of anxiety severity, using Stacked Sparse Autoencoder. They consider a 15 second recording too long for classification of anxiety, stating it may contain more than one emotion, and thus it explains why results didn't reach great accuracy. Such accuracy was obtained by segmentation of signal into 1s chunks.

Consequently, authors produced newer paper [7], where in addition to prediction based on SAM also examined prediction based on HAM-A, reaching better accuracy of 86.70% using Stack Sparse Autoencoder with large feature vector, consisting of 277 features.

Another study have worked on improving the results of the study in which the DASPS database has been developed [37]. An accuracy of 94.90% and 92.74% is achieved for two and four level anxiety classification, using RF classifier.

In the newest study [14], authors relied on transition behaviour instead of working with the direct features computed from the recorded signals. Highest accuracy of 83.8 % is obtained for both 2 and 4 level classification using k-NN.

Comparison of the existing methods using publicly available DASPS dataset is shown in figure 2.8.

Study	Model	Features	Labeling	#Features	#Classes	Accuracy (%)	Sensitivity	Specificity	F1 score
Baghdadi et. al [2020]	k-NN	Frequency DWT-based RMS	SAM self-recall after every stimuli situation	56	2	81.40	Not reported	Not reported	Not reported
		Time Hjorth		42	4	73.60			
	Stacked Sparse Autoencoder	Time Hjorth, Fractal Dimension Frequency Power, entropy Time-frequency Hilbert-Huang spectrum, DWT-based RMS	SAM self-recall after every stimuli situation	277	2	83.50	Not reported	Not reported	Not reported
					4	74.60			
			HAM-A assessed after all six stimuli situations		4	86.70	N: 0.85 L: 0.88 M: 0.61 S: 0.95	Not reported	Not reported
Chatterjee et. al [2023]	k-NN	Frequency Band power features	SAM self-recall after every stimuli situation	8	2	83.8	Not reported	Not reported	Not reported
		Time Hjorth Frequency Band power features, Engagement index		16	4	83.8	Not reported	Not reported	Not reported
Muhammad et. al [2022]	Random Forest	Frequency Rational asymmetry, Mean power, asymmetry index	SAM self-recall after every stimuli situation	10	2	88.37	N + L: 0.94 M + S: 0.79	Not reported	0.86
				8	4	79.86	N: 0.93 L: 0.52 M: 0.29 S: 0.87	Not reported	0.78
			HAM-A assessed after all six stimuli situations	9	2	94.90	N + L: 0.92 M + S: 0.96	Not reported	0.93
				10	4	92.74	N: 0.84 L: 0.91 M: 0.84 S: 0.96	Not reported	0.90

Figure 2.8: Comparison of ML methods proposed in the literature using DASPS dataset. Authors usually did not compute specificity in these papers, so values highlighted by blue color were additionally computed based on confusion matrices found in the papers. Sensitivity column contains sensitivities per class (N for normal, L for light, M for moderate, and S is for severe anxiety). Baghdadi et al. [7], Chatterjee et al. [14], Muhammad et al. [37].

2.4 Discussion

Research that is done in the field of anxiety detection can be categorized into two categories based on the anxiety type - state anxiety and trait anxiety. State anxiety is a normal response to a stressful or frightening situation that can be seen in all humans – both healthy and those suffering from an anxiety disorder. Research on state anxiety usually examines brain activity during acute anxiety induced by a psychotherapist in a safe environment. Then, EEG data are captured and analyzed. On the other hand, trait anxiety is considered a part of a person's personality that leads to recurring anxious behavior in everyday situa-

tions, which are generally not harmful. Trait anxiety is usually studied using resting state EEG recording, finding the differences between anxious and non-anxious groups. Current research not only tries to discriminate between anxiety and non-anxiety classes but also assesses the severity of anxiety. However, the problem with anxiety research is that the term "anxiety" varies in the literature – there is no agreed definition. Furthermore, in the former studies, "anxiety" (presumably state anxiety) is also often interchanged with "stress". Therefore, it has to be carefully assessed in terms of the protocol utilized for the EEG recording.

This chapter described various potential biomarkers related to anxiety. Regarding ERPs, the error-related negativity (ERN) seems promising as a robust trait marker of clinical anxiety. Regarding time domain features, Hjorth parameters are very simple to extract from EEG signals yet produce significant accuracies. Moving to the frequency domain features, delta-beta cross-frequency correlation is a promising measure of social anxiety disorder. Another frequency feature is the asymmetry index, a potential biomarker related to anxiety demonstrated by multiple studies. The amplitude of the beta band was also associated with the anxiety level of an individual. Regarding time-frequency features, alpha and beta band wavelet coefficients were found to be highly correlated with anxiety levels. Another study reports that time-frequency features obtained after a wavelet transform achieved the best rates in classification, among other methods. Partial directed coherence (PDC) was used as an effective connectivity feature, resulting in high classification accuracy when used with CNN and LSTM.

Four studies used a dataset consisting of individuals with no record of psychiatric disease [8, 14, 37, 3], one study used a mixed dataset of healthy and anxiety disorder patients [15], and one study did not specify [5]. Different headsets were used, with a density of 4, 14, and 32 channels. Surprisingly, even classification using a four-channel headset resulted in accuracy close to 90% [5]. The questionnaire used for labeling of data is different in almost every study. Classifying into more levels of granularity – i.e. severity of anxiety, resulting in lower accuracy in studies that compared the accuracy between different levels of granularity [15, 8, 37].

Only one anxiety dataset is publicly available and free to download, particularly the DASPS dataset with EEG recordings of 23 participants in anxiety induction trials. For more information about the dataset, see section 2.3.1. Because of availability, several studies used this dataset – results are compared in the table 2.8. Every study which used this dataset reported classification accuracies. Few studies also mention sensitivities. Sensitivity in this context refers to the probability that a subject with a positive anxiety test truly has anxiety. Lower accuracies are reported in multiclass classification as opposed to binary classification, where the highest accuracy of 92.74% achieved with sensitivities of 0.84 for normal anxiety, 0.91 for light anxiety, 0.84 for moderate anxiety, and 0.96 for severe anxiety, and F1 score of 0.9, which is not enough for a robust test. Specificities were not reported in either study. Specificity refers to the probability that a subject with a negative anxiety test truly does not have anxiety. Sensitivity and specificity are important measures to eliminate misdiagnoses and are heavily used in medicine.

To address shortcomings of previous studies, the next chapter proposes a novel anxiety detection based on machine learning methods, using microstates, and other features in time and frequency domain.

Chapter 3

Proposed Methodology

This chapter proposes a novel method of anxiety detection based on machine learning, addressing the shortcomings of previous studies. The DASPS dataset is used for this purpose. The ground truth is based on the HAM-A score. In the preprocessing stage, existing methods are used to remove undesirable elements from the data. The contribution of this work lies in incorporating various types of features, such as time series features, frequency features, time-frequency features, and microstates, into machine learning models. Classification is based on a two-phase classification consisting of three classifiers. It is important to note that every classifier performs feature extraction and feature selection independently, resulting in different feature sets. Finally, the result of the two-phase classification is the assignment into one of the four classes. The method proposed is shown in figure 3.1.

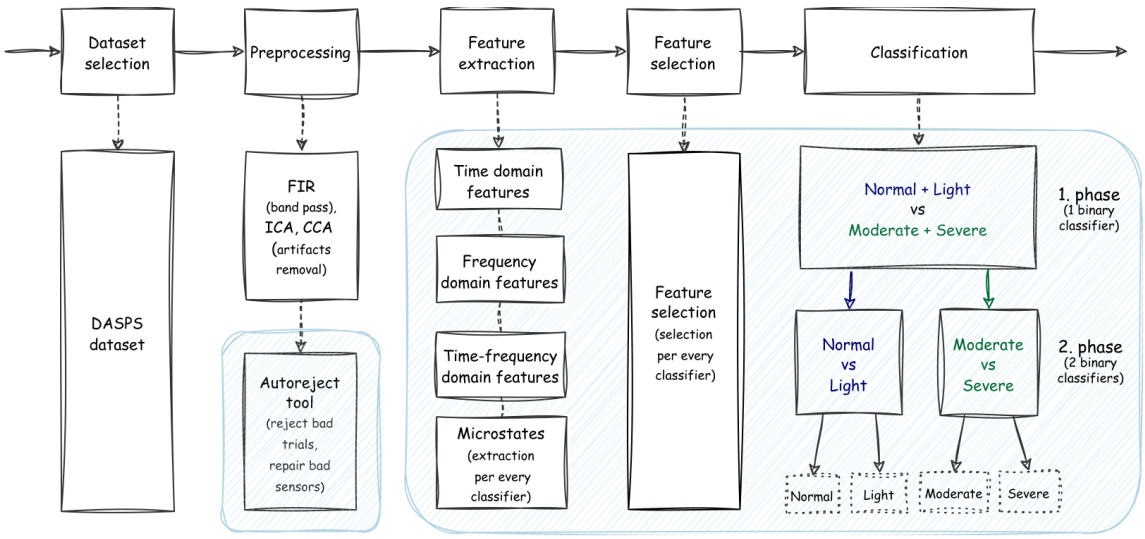

Figure 3.1: Figure showing proposal of a novel method of anxiety detection. The method incorporates various features into a two-phase classification process. In the first phase, the top-level model classifies trials into two classes – Normal + Light and Moderate + Severe. Then, in the second phase, further classification is done based on the assigned class from the first model. For example, if the assigned class from the first model is Normal + Light, the respective model in the second phase will further discriminate between Normal and Light classes. The same principle applies to the other alternative, i.e., the Moderate + Severe class. This work deals with areas highlighted in the blue rectangles.

3.1 Features

This section presents features extracted from the EEG signal for further classification tasks. These features consist of microstates, time series, frequency, and time-frequency features.

3.1.1 Microstates

The first set of features is based on microstates. Microstates are states or patterns of an EEG signal, lasting anywhere from milliseconds to seconds. Although many topographic maps can be obtained from an EEG signal, they are clustered based on similarity. Clustered microstates are then back-fitted to the EEG signal. Next, various statistical features are extracted. In particular, it is the microstates' duration, occurrence, recurrence, coverage, and transition probabilities. For a detailed diagram, see figure 3.2.

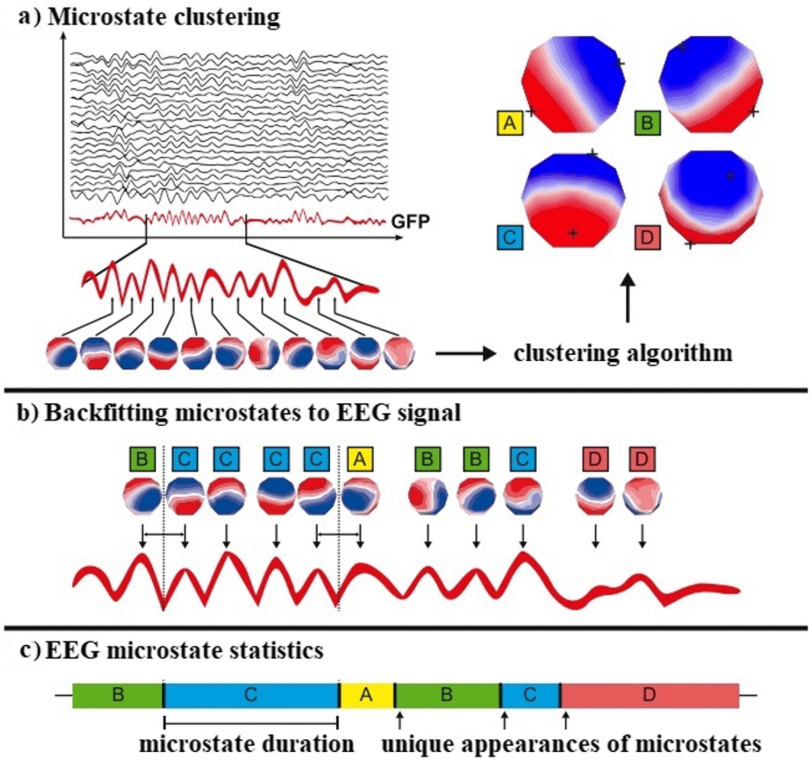

Figure 3.2: The figure shows microstate clustering, back-fitting of clustered microstates to EEG signal, and statistics based on microstates. a) The GFP curve, drawn in red, is obtained from the subjects' EEG signals. Then, from the topographic maps obtained based on the peaks of the GFP, microstate maps are obtained (A, B, C, and D) using a clustering algorithm. b) The back fitting procedure assigns microstate labels to EEG samples based on which microstate prototype they are most topographically similar to. c) From the EEG signal represented by a sequence of microstate labels, it is possible to calculate the statistical characteristics, such as microstates duration and the number of occurrences. The figure is taken from [31].

Let us move from the introduction of the microstates to the proposed method. The first step to obtaining microstates, Global Field Power (GFP), has to be computed. Then,

microstates from GFP peaks are clustered and back-fitted to the EEG signal. Subsequently, various features based on microstates are extracted, such as the occurrence of microstates, recurrence of microstates, duration of microstates, transition probabilities from one particular microstate to another, or coverage of microstates.

3.1.2 Time Series Features

Time series features can be further divided into univariate and bivariate categories. The univariate feature is computed from a single channel, whereas the bivariate feature is computed from two channels and thus captures the relationship between them.

Univariate Features

The following sections will describe univariate time series features that were selected, namely Mean, Standard deviation, Quantile, Kurtosis, Zero Crossings, Line Length, Hjorth Parameters, Root Mean Square, Peak-to-Peak Amplitude, Approximate Entropy, Hurst Exponent, Higuchi Fractal Dimension, Katz Fractal Dimension, SVD Entropy, and SVD Fisher Information.

Mean from a signal $\{x_i\}$ can be obtained using following formula:

$$\overline{x} = \frac{1}{n}\sum_{i=1}^{n} x_i \tag{3.1}$$

Standard Deviation from a signal $\{x_i\}$ can be obtained using following formula:

$$\sigma = \sqrt{\frac{1}{n}\sum_{i=1}^{n}(x_i - \overline{x})^2} \tag{3.2}$$

Quantile used in this particular case is 75% quantile. Quantile from a signal $\{x_i\}$ using $q = 0.75$ is a value below which 75% of the data falls.

Kurtosis can be defined using different ways. In this particular case, Pearson's definition is used. According to Person's definition, kurtosis is the fourth central moment μ_4, divided by the square of the variance:

$$\text{Kurtosis} = \frac{\mu_4}{\sigma^4} \tag{3.3}$$

Zero Crossings represents the number of positive crossings of a signal through zero.

Line Length is calculated as the sum of the absolute differences between each pair of adjacent points over a defined window [17]:

$$LL(n) = \frac{1}{K}\sum_{k=n-N}^{n} abs[x(k-1) - x(k)] = \frac{L(n)}{K} \tag{3.4}$$

where $LL(n)$ is the normalized line length value at discrete time index n, $L(n)$ is the running sum of distances between successive points within the sliding window of size $N, x[k]$ is the

data sequence value at the k^{th} sample, K is the normalization constant, N is the sliding windows length and *abs* stands for absolute value. Finally, $LL(n)$ is computed for each sample and then the average, representing the final feature.

Hjorth Parameters were already described in section 2.1.3.

Root Mean Square (RMS) is defined by following formula:

$$RMS = \sqrt{\frac{1}{n}\left(x_1^2 + x_2^2 + \cdots + x_n^2\right)} \tag{3.5}$$

Peak-to-Peak Amplitude represents the difference between the maximum peak and the minimum peak contained in the signal.

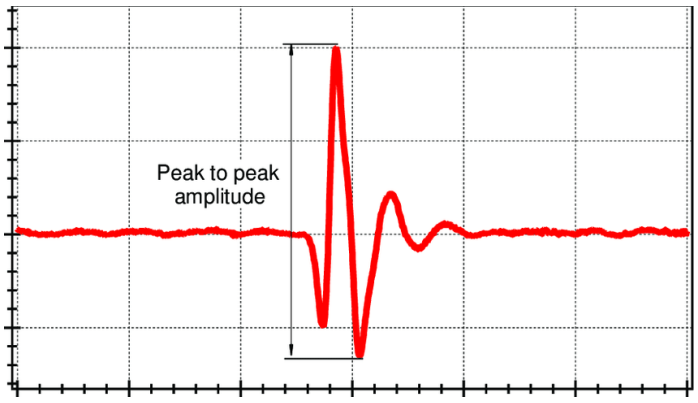

Figure 3.3: The figure shows the original signal and the signal produced by applying the Teager-Kaiser Energy operator. The figure is taken from [23].

Approximate Entropy is a measure of system complexity. Lower values mean higher self-similarity in the time series [41]. Let EEG signal be defined as $x(1), x(2), \ldots, x(N)$ and m dimensional vectors starting with i^{th} point:

$$\begin{aligned} &X(i) = [x(i), x(i+1), \ldots, x(i+m-1)] \\ &X(j) = [x(j), x(j+1), \ldots, x(j+m-1)] \\ &i, j = 1 < N - m + 1; j \neq i \end{aligned} \tag{3.6}$$

and Approximate Entropy defined as:

$$ApEn(m, r, N) = \phi^m(r) - \phi^{m+1}(r) \tag{3.7}$$

where m is length of EEG segment, r is the tolerance value, N is total length of EEG signal, and function $\phi^m(r)$:

$$\phi^m(r) = (N - m + 1)^{-1} \sum_{i=1}^{N-m+1} \ln\left[C_i^m(r)\right] \tag{3.8}$$

is the average of the natural logarithms of the function $C_i^m(r)$, which is the probability that any vector $x_m(j)$ is within r of $x_m(i)$:

$$C_r^m(i) = \frac{B_i}{N-m+1} \tag{3.9}$$

where B_i is the number of vectors $x_m(j)$ within r of $x_m(i)$. Let A_i be the number of vectors $x_{m+1}(j)$ within r of $x_{m+1}(i)$, then:

$$\begin{aligned} &C_r^{m+1}(i) = \tfrac{A_i}{N-m} \\ &\phi^{m+1}(r) = (N-m)^{-1} \textstyle\sum_{i=1}^{N-m} \ln\left[C_i^{m+1}(r)\right] \end{aligned} \tag{3.10}$$

Hurst Exponent ranges between 0 and 1, and is defined as:

$$H = \frac{\log(R(T)/S(T))}{\log(T)} \tag{3.11}$$

where $R(T)$ is a difference between maximum and minimum values of the signal during time interval T, and $S(T)$ is the standard deviation of the EEG signal.

Higuchi Fractal Dimension is used to quantify the complexity and self-similarity of the signal. Let represent EEG signal as $X(1), X(2), \ldots, X(N)$, and construct a new time series, X_k^m as follows:

$$X_m^k = X(m), X(m+k), X(m+2k), \ldots, X\left(m + \left[\frac{N-m}{k} \cdot k\right]\right) (m = 1, 2, \ldots, k) \tag{3.12}$$

where m indicate initial time and and k indicate interval time respectively. In the case of $k = 4$ and $N = 1000$, for example, four time series are produced:

$$\begin{aligned} &X_1^4 : X(1), X(5), X(9), \ldots, X(993), X(997) \\ &X_2^4 : X(2), X(6), \ldots, X(998) \\ &X_3^4 : X(3), X(7), \ldots, X(999) \\ &X_4^4 : X(4), X(8), \ldots, X(1000) \end{aligned} \tag{3.13}$$

Then, length of the curve, X_m^k is defined as follows:

$$L_m(k) = \left\{ \left(\sum_{i=1}^{\left[\frac{N-m}{k} \cdot k\right]} |X(m+ik) - X(m+(i-1) \cdot k| \right) \frac{N-1}{\left[\frac{N-m}{k} \cdot k\right] \cdot k} \right\} \Big/ k \tag{3.14}$$

Finally, the length of the curve for the time interval k, $L(k)$, is calculated as the mean of the k values $L_m(k)$ for $m = 1, 2, \ldots, k$. [1]

Katz Fractal Dimension is derived directly from the waveform. The fractal dimension of a curve can be defined as:

$$D = \frac{\log(n)}{\log(d/L) + \log(n)} \tag{3.15}$$

where L is the total length of the curve or sum of distances between successive points, and d is the diameter estimated as the distance between the sequence's first point and the sequence's point that provides the farthest distance. [18]

SVD (Singular Value Decomposition) Entropy is defined as [42]:

$$H = -\sum_{i=1}^{N} \overline{\sigma}_i \log \overline{\sigma}_i \tag{3.16}$$

where $\overline{\sigma_i}$ denotes normalized singular value:

$$\overline{\sigma}_i = \frac{\sigma_i}{\sum_i \sigma_i} \tag{3.17}$$

SVD (Singular Value Decomposition) Fisher Information is defined as:

$$F_{\text{SVD}} = \sum_{i=1}^{N-1} \frac{(\overline{\sigma}_{i+1} - \overline{\sigma}_i)^2}{\overline{\sigma}_i} \tag{3.18}$$

where $\overline{\sigma_i}$ denotes normalized singular value:

$$\overline{\sigma}_i = \frac{\sigma_i}{\sum_i \sigma_i} \tag{3.19}$$

Teager-Kaiser Energy is a nonlinear quadratic operator to measure the real physical energy of a system E_n:

$$E_n = x_n^2 - \left(x_{(n+1)}\right) * \left(x_{(n-1)}\right) \tag{3.20}$$

where x_n is a discrete time signal and n is the discrete time index. This operator is capable of tracking instantaneously-varying special patterns. [19]

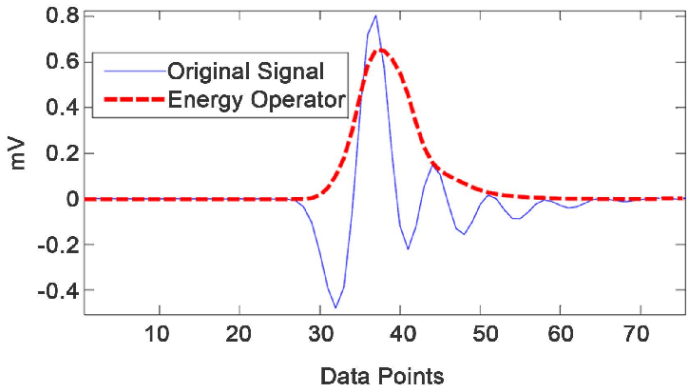

Figure 3.4: The figure shows the original signal and the signal produced by applying the Teager-Kaiser Energy operator. The figure is taken from [19].

Bivariate Features

The following sections will describe selected bivariate time series features, namely Maximum Linear Cross-Correlation, Non-Linear Interdependence, Phase-Locking Value, and Correlation Coefficients.

Maximum Linear Cross-Correlation is a measures similarity of two signals $\{x_i\}$ and $\{y_i\}$. It can be quantified by using the maximum of a normalized cross-correlation function as a measure for lag synchronization:

$$C_{\max} = \max_{\tau} \left\{ \left| \frac{C_{xy}(\tau)}{\sqrt{C_{xx}(0) \cdot C_{yy}(0)}} \right| \right\} \tag{3.21}$$

where $C_{xy}(\tau)$ is linear cross-correlation function. C_{max} is confined to the interval $[0, 1]$ with high values indicating that the two signals have a similar course in time (though possibly shifted by a time lag τ). In contrast, dissimilar signals will result in values close to zero. [36]

Non-Linear Interdependence as a measure for generalized synchronization between two EEG signals $\{x_i\}$ and $\{y_i\}$ is calculated after reconstruction of the state space trajectories $\{\vec{x}_i\}$ and $\{\vec{y}_i\}$ for these signals. Let α_{ij} and β_{ij} with $j = 1, \ldots, k$ denote the time indices of the k nearest neighbours in state space of $\vec{x}_i$ and $\vec{y}_i$, respectively. For each $\vec{x}_i$ the squared mean Euclidean distance to its k nearest neighbours is given by

$${}^{\mathrm{x|y}}S = \frac{1}{M} \sum_{i=1}^{M} \frac{{}^{\mathrm{x}}R_i^{(k)}}{{}_{\mathrm{x|y}}R_i^{(k)}} \tag{3.22}$$

and

$${}^{\mathrm{x|y}}H = \frac{1}{M} \sum_{i=1}^{M} \log \frac{{}^{\mathrm{x}}R_i^{(M)}}{{}_{\mathrm{x|y}}R_i^{(k)}} \tag{3.23}$$

with

$${}^{\mathrm{x}}R_i^{(M)} = \frac{1}{M-1} \sum_{j=1, j \neq i}^{M} (\vec{x}_i - \vec{x}_j)^2 \tag{3.24}$$

${}^{y|x}S$ and ${}^{y|x}H$ are defined accordingly. Both measures yield high values for high degrees of non-linear interdependence and low values for independent time series. While ${}^{x|y}S$ is restricted to the interval $[0, 1]$, ${}^{x|y}H$ is not normalized and might also have slightly negative values. [36]

Phase Locking Value quantifies locking between the phases of the signals from two distinct electrodes. For each channel i, extract instantaneous phase $\phi_i^a(t)$ of the analytical signal $x_i^a(t)$ of the time series $x_i(t)$. Then, for each pair (i, j) of channels, compute the modulus of the time-averaged phase difference mapped onto the unit circle [47]:

$$PLV_{ij} = \left| \frac{1}{T} \sum_{t} e^{i\left(\phi_i^a(t) - \phi_j^a(t)\right)} \right| \tag{3.25}$$

Correlation Coefficients in the time domain between pair of EEG channels, using Pearson product-moment correlation coefficients. The input EEG signal is first standardized, then the correlation coefficient matrix is calculated. The relationship between the the correlation coefficient matrix, R, and the covariance matrix, C, is:

$$R_{ij} = \frac{C_{ij}}{\sqrt{C_{ii} C_{jj}}} \tag{3.26}$$

where values of R are between -1 and 1, inclusive. Eigenvalues of the correlation matrix are calculated too.

3.1.3 Frequency Features

Frequency features consist of Band Power, Asymmetry Index, Correlation Coefficients (from power spectra), Decorrelation Time, Spectral Edge Frequency, and Spectral Slope.

Band Power was already described in section 2.1.4.

Asymmetry Index was already described in section 2.1.4.

Correlation Coefficients in the frequency domain, obtained from the power spectrum. The only difference of this feature with the time-domain variant is that for input data power spectrum is used, which is obtained using Welsch's method. All other details are the same as in the time domain variant; See 3.1.2.

Decorrelation Time is defined as the time of the first zero crossing of the autocorrelation sequence of a given EEG signal. If the decorrelation time is lower, the signal is less correlated. The autocorrelation function is computed using the FFT of the signal. [50]

Spectral Edge Frequency is another measure obtained from the power spectrum. In a typical EEG signal, most of the power is contained within the frequency band from 0 Hz up to 40 Hz : $P_{40\ \mathrm{Hz}} \approx P$. As a characterizing measure for the power distribution, the so-called spectral edge frequency can be used, which is defined as the minimum frequency up to which 50% the spectral power up to 40 Hz is contained in the signal [36]:

$$f_{50} = \min \left\{ f^* \mid \sum_{f=0\ \mathrm{Hz}}^{f^*} p_f > P_{40\ \mathrm{Hz}} \cdot 0.50 \right\}. \tag{3.27}$$

Spectral Slope is estimated using linear regression of the power spectral density in the log-log scale. Additionally, an intercept is used as a feature, too. Figure 3.5 shows a log-log scale with an estimated spectral slope.

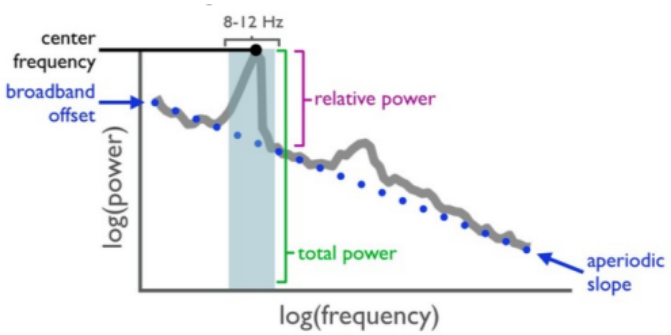

Figure 3.5: The figure shows the spectral slope on the power-spectral-density log-log graph. The spectral slope is estimated using linear regression and shown as a dotted line. The figure is taken from [20].

3.1.4 Time-Frequency Features

The last category is for time-frequency features, which consist of only the Energy of Wavelet Decomposition Coefficients.

Energy of Wavelet Decomposition Coefficients is obtained after wavelet transform. For more information about wavelet transform, see 2.1.5. Wavelet used for this features is Daubechies 4 (db4). After DWT (Discrete Wavelet Transform), coefficients are obtained. Finally, energy is computed as the sum of the square of the absolute values of those coefficients.

3.2 Feature Selection

The next step is to perform feature selection based on already computed features. Features are normalized before performing the feature selection step to have a similar scale. This ensures that all features contribute equally to the model and prevents features with larger values from dominating the model.

Various feature selection methods were tested: Ridge regression, Lasso regression, Correlation, and Sequential Feature Selection. Ridge regression with Recursive feature elimination (RFE) is used as it showed the best classification performance on the final model, selecting the most relevant features.

Ridge regression is linear least squares with L2 regularization. It adds "squared magnitude" of coefficient as penalty term to the loss function:

$$\text{Loss} = \text{Error}(Y - \widehat{Y}) + \lambda \sum_{1}^{n} w_i^2 \tag{3.28}$$

However, as we have a classification problem, a classification variant is used instead of regression. The ridge classifier converts binary targets to $\{-1, 1\}$ and then treats the problem as a regression task, optimizing the same objective as above.

When the model is fitted on the provided data, based on the coefficients assigned to every feature, the RFE step is performed. RFE aims to select features by recursively considering smaller and smaller sets of features. First, the estimator is trained on the initial set of features, and the importance of each feature is obtained. Then, the least important feature is pruned from the current set of features. The least important feature is the one having the smallest coefficient, thus not contributing to the final decision. The procedure is recursively repeated on the pruned set until the desired number of features to select is eventually reached. In this case, the number of features to select is set experimentally based on the classification performance.

3.3 Classification

The proposed method consists of a two-phase classification process, using SVM models. In the first phase, the top-level model classifies trials into two classes – Normal + Light and Moderate + Severe. Then, in the second phase, further classification is done based on the assigned class from the first model. For example, if the assigned class from the first model is Normal + Light, the respective model in the second phase will further discriminate between Normal and Light classes. The same principle applies to the other alternative, i.e., the Moderate + Severe class. For more information about the method, see figure 3.1.

Chapter 4

Implementation

This chapter presents tools used to implement the proposed method, including preprocessing, calculation of features, feature selection, classification models, and hyper-parameter tuning of the models.

4.1 Tools

This section lists the tools that were used to implement the proposed method. For the implementation, Python programming language was chosen. Pandas[1] is used to manipulate data. Calculations related to vectors, matrices, and multidimensional arrays are done using NumPy[2]. For machine learning and statistical calculations, scikit-learn[3] and SciPy[4] is used. Matplotlib[5] is used for data visualization. For loading EEG data from MATLAB format, mat73[6] is used, as the dataset is in MATLAB 7.3 .mat format. MNE[7] is an open-source Python package for exploring, visualizing, and analyzing human neurophysiological data from various sources, such as EEG or MEG. This toolbox was used for easier manipulation with EEG epoched data and other helper functions. Some features were extracted using MNE-Features[8] package. This package implements various univariate and bivariate, time, and frequency features. Epochs rejection and repairment is done using Autoreject[9] package. At the start of the work, the first hands-on with the data to check the validity by visual inspection was done using MATLAB's EEGLAB[10] plugin.

Data Inspection

To ensure validity of the downloaded DASPS dataset, data were first loaded and plotted using Matlab software and the EEGLAB package. Data from the first participant are plotted in figure 4.1.

[1] https://pandas.pydata.org
[2] https://numpy.org
[3] https://scikit-learn.org
[4] https://scipy.org
[5] https://matplotlib.org
[6] https://pypi.org/project/mat73
[7] https://mne.tools
[8] https://mne.tools/mne-features
[9] https://autoreject.github.io
[10] https://eeglab.org

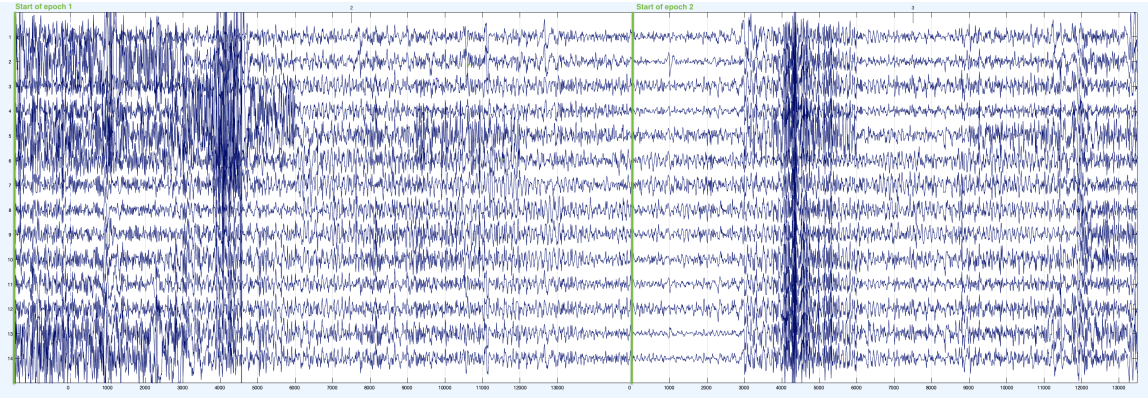

Figure 4.1: The figure shows the EEG data of a participant in the DASPS database during the first trial. There are visible muscle artifacts that need to be cleaned. Due to reported high HAM-A and SAM scores, anxiety in the subject was elicited. The x-axis shows time (milliseconds) per epoch, and the y-axis shows channels. Two epochs of length 15 seconds are shown – the first is a recitation by a psychotherapist trying to induce anxiety, and the second is the self-recall by the subject. The plot was created using Matlab EEGLAB software.

4.2 Preprocessing

The DASPS dataset contains both raw and preprocessed versions of the data. The raw data are available in ".edf" and ".mat" format, while preprocessed data are only available in ".mat" format. Preprocessed data were denoised by cutting only the relevant sub-band of EEG signals and removing ocular and muscular artifacts. A 4-45 Hz Finite impulse response (FIR) pass-band filter was used for sub-band extraction. Artifacts were removed using the EEGLAB toolbox by the authors of the dataset, and are summarized in the next two paragraphs.

Muscular artifacts were removed using the implementation of BSSCCA Canonical Correlation Analysis (CCA), which projects the observed EEG data into maximally autocorrelated components. The criterion used is "emg_psd", which considers the components whose average power ratio in the typical EEG and EMG bands is below a certain threshold to be EMG-related. The power estimator used is a Hamming-windowed Welch periodogram.

Ocular artifacts were corrected using the iWASOBI blind source separation algorithm for autoregressive sources and the criterion "eog_fd", which marks the components with smaller fractal dimensions as artifactual. Conceptually, components with low fractal dimensions are composed of few low-frequency components, which is often the case of ocular activity. Therefore it is a suitable criterion for detecting ocular (EOG) components.

All this preprocessing steps were performed by the authors of the dataset. However, after visualizing the data, there were still some artifacts left. Because of this, there is a need to perform another artifact rejection procedure. For this, the Python framework Autoreject was used. The Autoreject framework was used for the rejection of bad epochs and artifacts. All algorithm steps are fully automated; that is also why the authors named it Autoreject. A total of 35 epochs were further removed as part of the rejection procedure, therefore final dataset contains 241 epochs. In addition, epochs that were not removed are repaired. This preprocessing step should help with cleaning of data for the latter feature extraction step that will follow.

4.3 Features

Every feature used is initialized from the base class `Feature`. This class contains method `compute_feature()`, and all features inherited from parent class `Feature` must implement this method. This method is used to compute the feature, as the name suggests.

Regarding the time needed to calculate features for the whole dataset, it takes around 10 minutes in parallel mode on 8-core AMD RYZEN 7 5800X @ 3.8GHz with 32 GB of RAM.

The following sections outline the implementation details of the features that are used.

Microstates

The number of microstates is an important parameter when extracting the microstates. In the review study of "EEG microstates as a tool for studying the temporal dynamics of whole-brain neuronal networks" [35], authors discussed various aspects of microstates, along with the number of cluster maps to extract. The authors mention that several initial studies that used the k-mean clustering approach determined that the optimal number of cluster maps across subjects is four. The global variance (GEV) that these four cluster maps explain varies between reports, ranging from 65 to 84%. On the other hand, the authors mention that another study reported that fifteen clusters were needed to explain approximately 80% of the variance. The authors suggest that the most appropriate choice for the number of cluster maps may not necessarily correspond to the "true" number of cluster maps. It may instead result from a pragmatic compromise between the needs for specificity - which typically benefits from increasing the number of maps – and generalizability, which typically benefits from a relatively low number of maps.

To help find the number of microstates to extract, the Calinsky-Harabasz score was used. Calinsky-Harabasz is also known as the Variance Ratio Criterion. The score is defined as the ratio of the sum of between-cluster dispersion and of within-cluster dispersion. The higher the score, the higher the dispersion between clusters and the lower dispersion within clusters. The final number of microstates selected is chosen to be 7. Scores for 2-7 clusters are visualized in figure 4.2. It is visible that score for 7 clusters represents the local peak. The GEV (Globally Explained Variance) for seven clusters is 83.91%, a sufficiently high variance that explains the data.

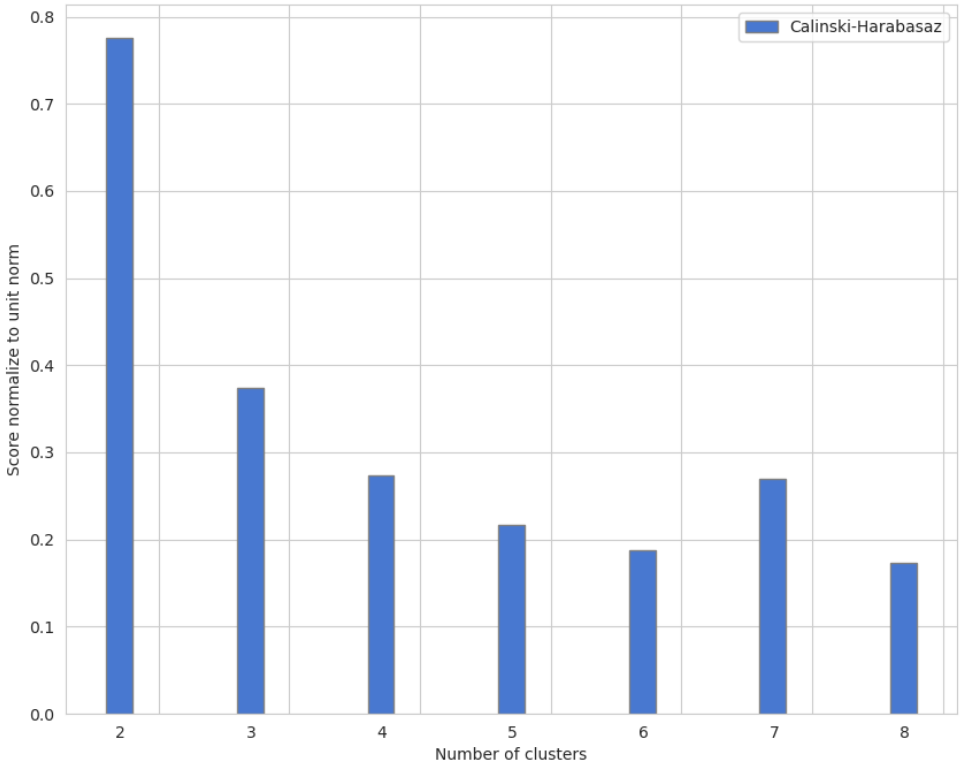

Figure 4.2: The figure shows the number of clusters with their corresponding Calinsky-Harabasz score.

Microstates are extracted for every model, as the data set differs in every model. Figure 4.3 shows extracted microstates for all models in the two-phase process. The first phase consists of a model where all data are present; the second phase consists of Normal + Light data, and the last model consists of Moderate + Severe data.

Looking at the figure, some of the extracted microstates can be instantly recognized based on their similarity, compared with usually extracted microstates in the other literature. For example, microstates "3" and "6" for all data (Normal + Light + Moderate + Severe), which represent left-frontal to right-posterior and right-frontal to left-posterior topographies, respectively.

However, some microstates might account for artifacts left in the data, for example, "5" in the Moderate + Severe case. Fortunately, as feature selection is included in the classification pipeline, it will only select features that contribute to the classifier's performance, thus removing unnecessary features. Artifacts do not contribute to the classification. Because of this, such features extracted from "bad" microstates, which do not represent brain state but rather some artifact, will not be included in the final set of selected features.

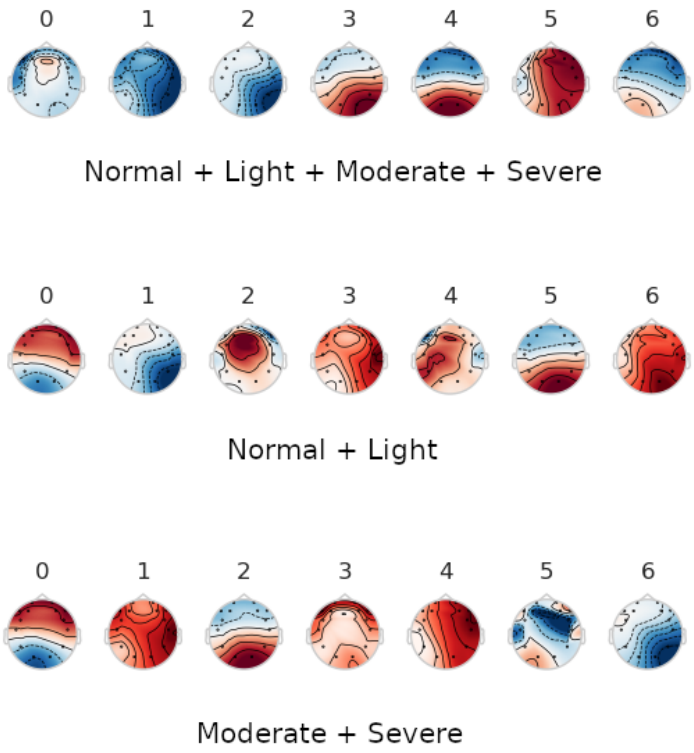

Figure 4.3: The figure shows microstates extracted in the first phase, where all data are present, and subsequently extracted microstates for the second phase, for the Normal + Light data, and for the Moderate + Severe data.

Based on the extracted microstates, various statistical features were extracted. Namely, microstates durations, the occurrence of microstates in the given epochs, coverage of the microstate over the epoch, and transition probabilities between microstates. Besides microstates, other features were extracted and are explained in the next section.

Band Power

Another extracted feature is band power. This feature is explained in section 2.1.4. Band power is computed using Welch's method. It is computed as the average over power spectral densities in the given frequency band. Band power is calculated for delta, theta, alpha, beta, and gamma bands. This feature is implemented in `BandPower(Feature)` class.

Asymmetry Index

Another extracted feature is the asymmetry index between pairs of EEG channels for the alpha band (8-12 Hz). This feature is already explained in section 2.1.4. Regarding implementation, power spectral density is estimated using Welch's method. Then, only frequen-

cies in the alpha range are kept. Next, the mean power in the alpha band is calculated. The asymmetry index is finally computed as the difference in the mean power between pair of channels, divided by their sum. The feature is implemented in `AsymmetryIndex(Feature)` class.

MNE-Features

MNE-Features is a library in Python for feature extraction from M/EEG data. It implements various univariate and bivariate features easily integrated with the MNE toolbox. All features proposed to use (see Proposed Methodology chapter) that were not mentioned previously in this chapter are extracted using this library.

All features calculated by this library used default values for all parameters except the power and energy of the frequency band. These two needed a little tweak; by default, they are defined to work up to 100 Hz. However, the sampling frequency of the data is 128 Hz, and this calculation only works for frequencies that are less than half of the sampling frequency. So the arguments of these features are updated to calculate it only for the delta, theta, alpha, beta, and gamma band. All MNE-Features are wrapped under a class named `MNEFeatures(Feature)`.

4.4 Model Development

Feature selection

The next step is to perform feature selection based on already computed features. Features were normalized before performing the feature selection step to have a similar scale. It also significantly speeded up the model fitting to the data.

Ridge regression with Recursive feature elimination (RFE) is used as it showed the best classification performance on the final model, therefore selecting the most relevant features. Feature selection steps used are implemented as part of the scikit-learn package – cross-validation variant of Ridge classifier (`sklearn.linear_model.RidgeClassifierCV`) and RFE (`sklearn.feature_selection.RFE`).

Classification

Various classification models were examined to see how they compare in classification between anxiety levels. The main focus was on Support Vector Machine (SVM) and Random Forests (RF). Besides these, other models such as Decision Tree, K-Nearest Neighbours, Logistic Regression, or Multi-layer perceptron (MLP) were tested.

Random Forests is not working well with imbalanced datasets, which DASPS dataset is. Thus, the RF model always preferred to classify the most occurring class. As already mentioned, other models were tested, but as SVM showed first some highly positive results, the main focus stayed on SVM.

The next section describes tuning of hyper-parameters, which improved classification performance of the models.

Hyperparameter Tuning

At the beginning of experiments, all models were based on C-Support Vector Classification (`sklearn.svm.SVC`), with the C parameter set to default value of 1.0. However, as shown

later, Nu-Support Vector Classification (`sklearn.svm.NuSVC`) reached higher classification performance in one of the models described in the next paragraph.

One of the models in the two-phase classification resulted in better classification results when using the already mentioned Nu-Support Vector Classification. In particular, it is in the second phase of the Normal and Light classification. The optimized parameter `nu` improved the classifier's overall performance. For the tuning of the hyperparameter, Grid Search was used to find the best value of the parameter `nu`, which is 0.1. The parameter `nu` represents an upper bound on the fraction of margin errors and a lower bound of the fraction of support vectors relative to the total number of training examples. For example, if `nu` is set to 0.1, there is a guarantee to find at most 10% of the training examples being misclassified (at the cost of a small margin, though) and at least 10% of the training samples being support vectors. The value is in the interval $(0, 1]$.

Another parameter that was tuned is `class_weight`, where every class is assigned the weight, which penalizes the class and is useful when the dataset is unbalanced. In this case, it was shown that the best results are obtained when setting weights based on the proportion of the class.

Chapter 5

Results

This chapter summarizes the results of the classification of the proposed method. For the evaluation of performance, 10-fold cross-validation was used. Every fold is made by preserving the percentage of samples for each class. It is important to mention that if participants' epochs are present in the training fold, they are never part of the testing fold. This is to preserve that the classifier does not classify anxiety based on the similarity of EEG data from the same participant but generalizes over differences that appear with people having anxiety.

5.1 Classification

Best results for all types of classification were obtained using SVM with linear kernel. Because of the class imbalances in the dataset, weights for the classifier were set based on the class proportion to penalize classes with a higher number of data points. This helps the classifier model decision boundary more accurately, mitigating class imbalances.

It is important to mention that every phase has its unique feature set to maximize classification performance. In the case of one particular feature, microstates, not only a different set of statistical features is selected, but also extracted microstates are different, as the set of EEG data is different for every model (e.g., the model that discriminates normal and light class contains only epochs trials labeled as normal or light and therefore microstates has to differ).

Next section describes classification results from the first phase, binary classification between the Normal + Light class and Moderate + Severe class.

5.1.1 I. phase

The first phase is to classify anxiety into two classes. As there are four classes initially, Normal and Light cases are grouped together, and the same is for Moderate and Severe.

The best results for binary classification were obtained using SVM with a linear kernel. Accuracy reached 98%, with a sensitivity of 0.95 and 1.00, specificity of 1.00 and 0.95, and F1 score of 0.97 and 0.99 for Normal + Light and Moderate + Severe classes, respectively. A confusion matrix is shown in figure 5.1. Other models, such as Random Forests or MLP, were tried, but SVM outperformed them. The main problem in Random Forest is an imbalance between classes, which confirms that the Random Forest is prone to prefer classes with more samples in the training set.

The best results were obtained by using a combination of various features. Selected features, with their respective coefficients assigned by the classifier, are shown in figure 5.2. When using only a single feature type for classification, accuracy never reached over 70% for any feature type.

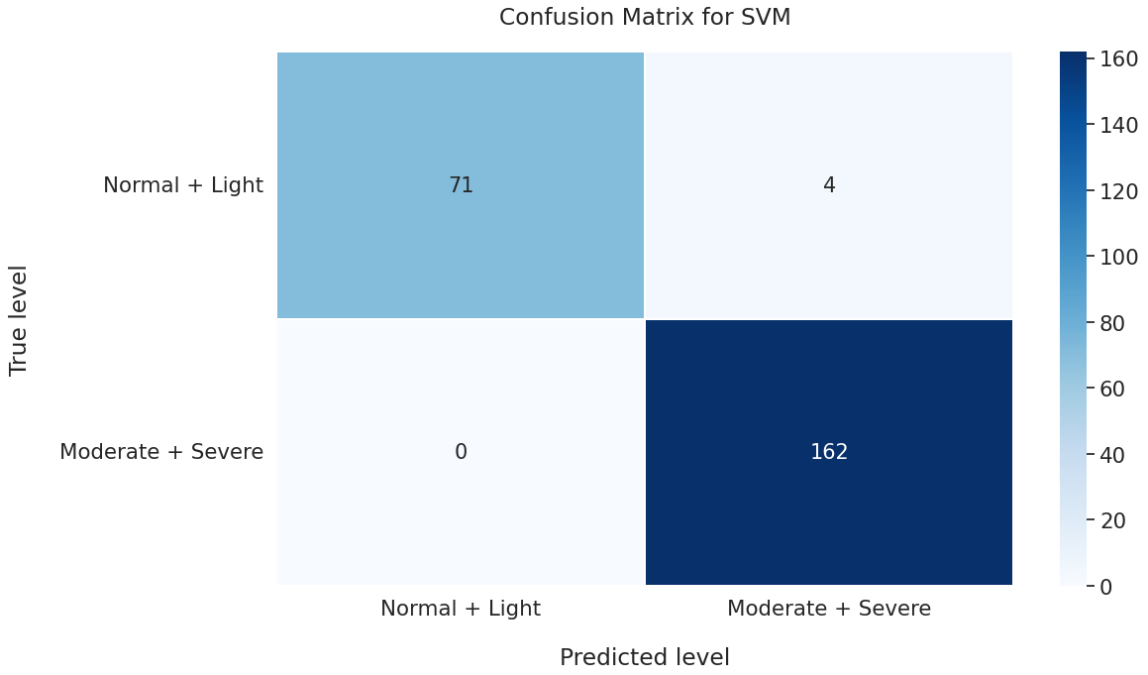

Figure 5.1: Confusion matrix for Normal + Light and Moderate + Severe classes.

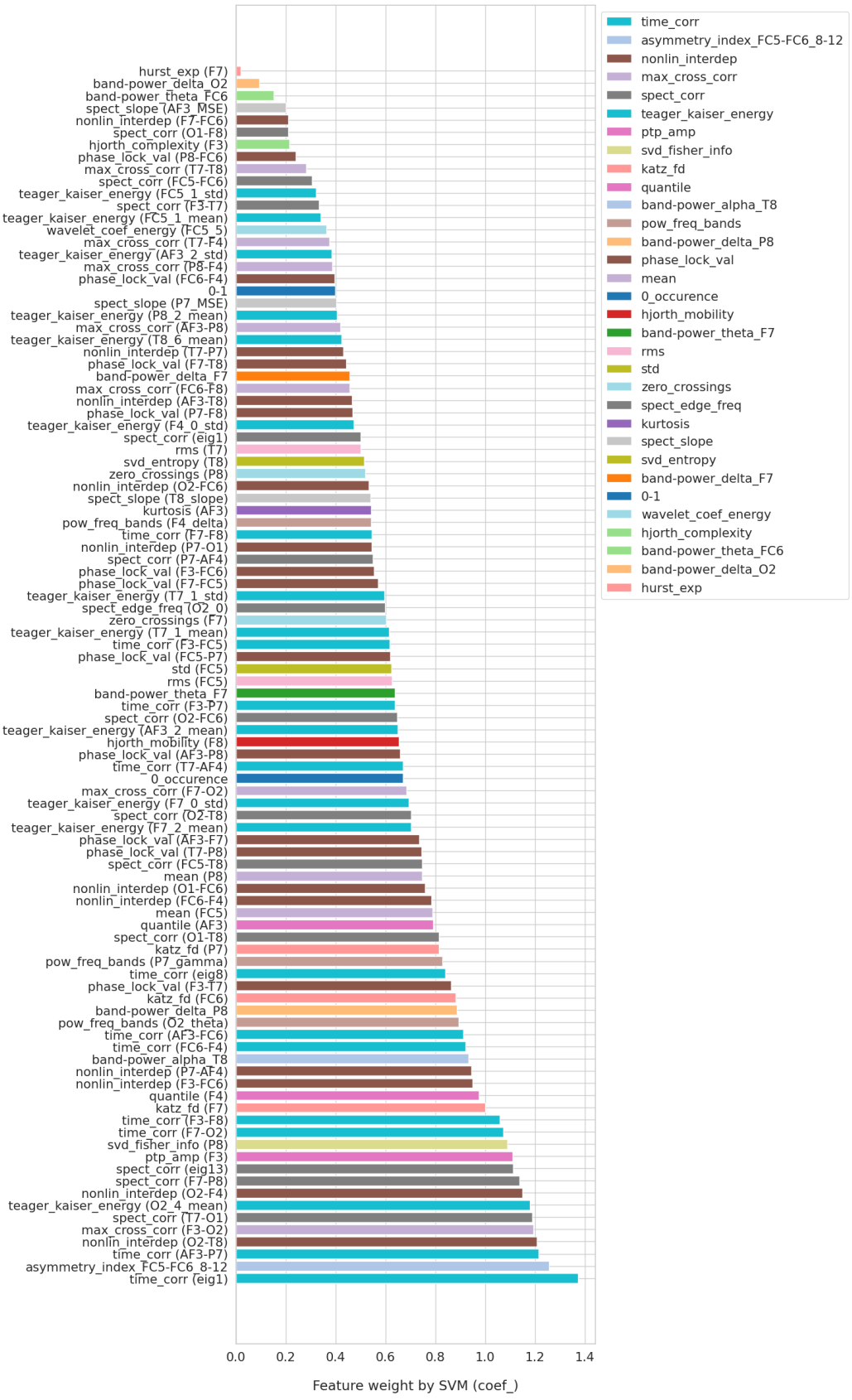

Figure 5.2: Selected features with weights by the SVM model (Normal + Light and Moderate + Severe). See Appendix B.

5.1.2 II. phase

The second phase consists of two models. The first model is to discriminate between Normal and Light classes, and the second is between Moderate and Severe classes. Results are described in the following sections.

Normal and Light

The best results for binary classification between Normal and Light classes were obtained using SVM with linear kernel again. Accuracy reached is 96%, the sensitivity of 0.87 and 1.00, specificity of 1.00 and 0.87, and F1 score of 0.93 and 0.97 for Normal and Light classes, respectively. A confusion matrix is shown in figure 5.3. Other models were tried, too, but were outperformed by SVM.

The best results were obtained by using a combination of various features. Selected features, with their respective coefficients assigned by the classifier, are shown in figure 5.4.

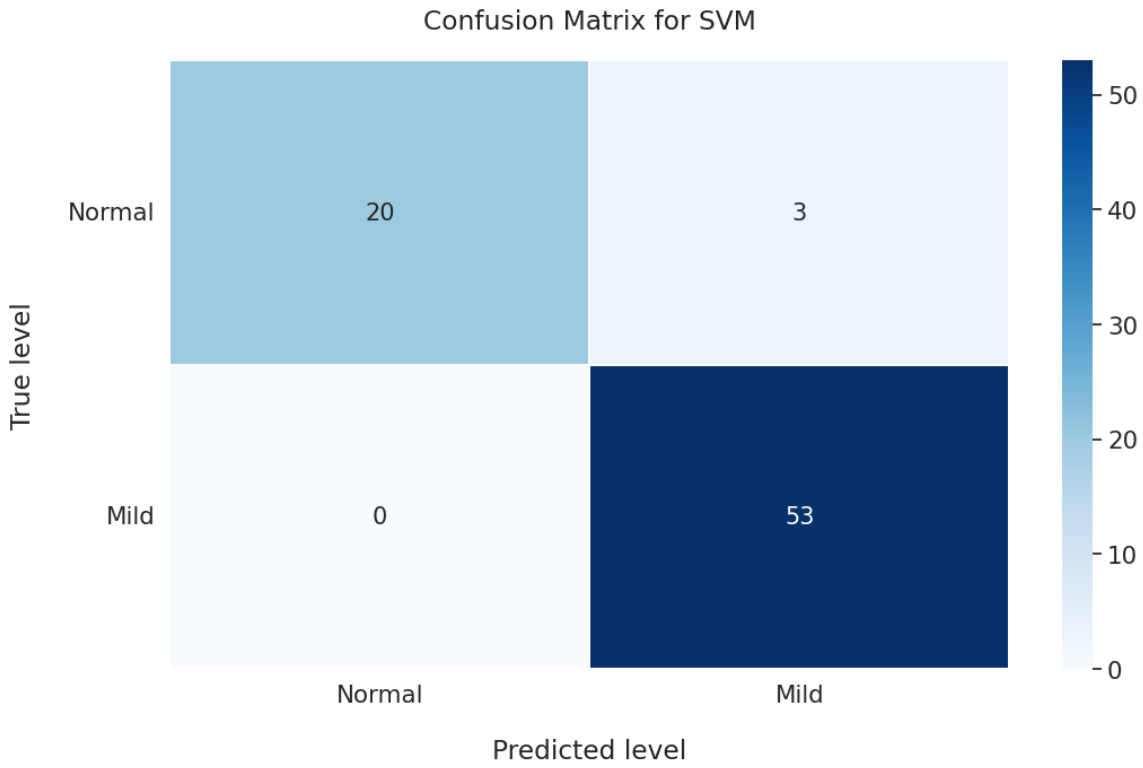

Figure 5.3: Confusion matrix for Normal and Light classes.

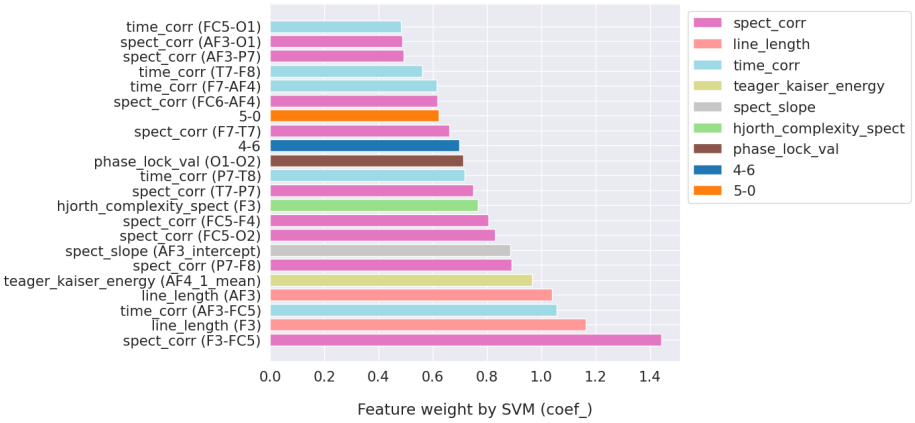

Figure 5.4: Selected features with weights by the SVM model (Normal vs. Light). Feature abbreviations are described in Appendix B.

Moderate and Severe

The best results for binary classification between Moderate and Severe classes were obtained again using SVM with linear kernel. Accuracy reached 99%, with a sensitivity of 0.97 and 0.99, specificity of 0.99 and 0.97, and F1 score of 0.97 and 0.99 for Moderate and Severe classes, respectively. A confusion matrix is shown in figure 5.5. Other models were tried, too but were outperformed by SVM. Selected features, with their respective coefficients assigned by the classifier, are shown in figure 5.6.

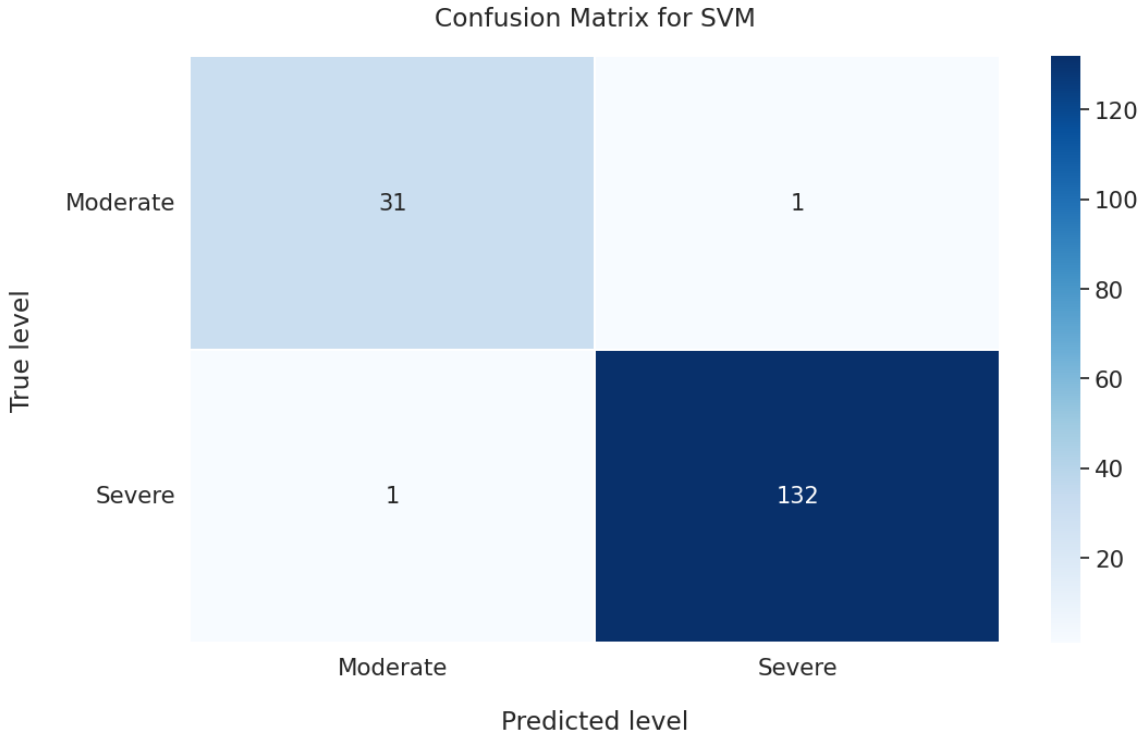

Figure 5.5: Confusion matrix for Moderate and Severe classes.

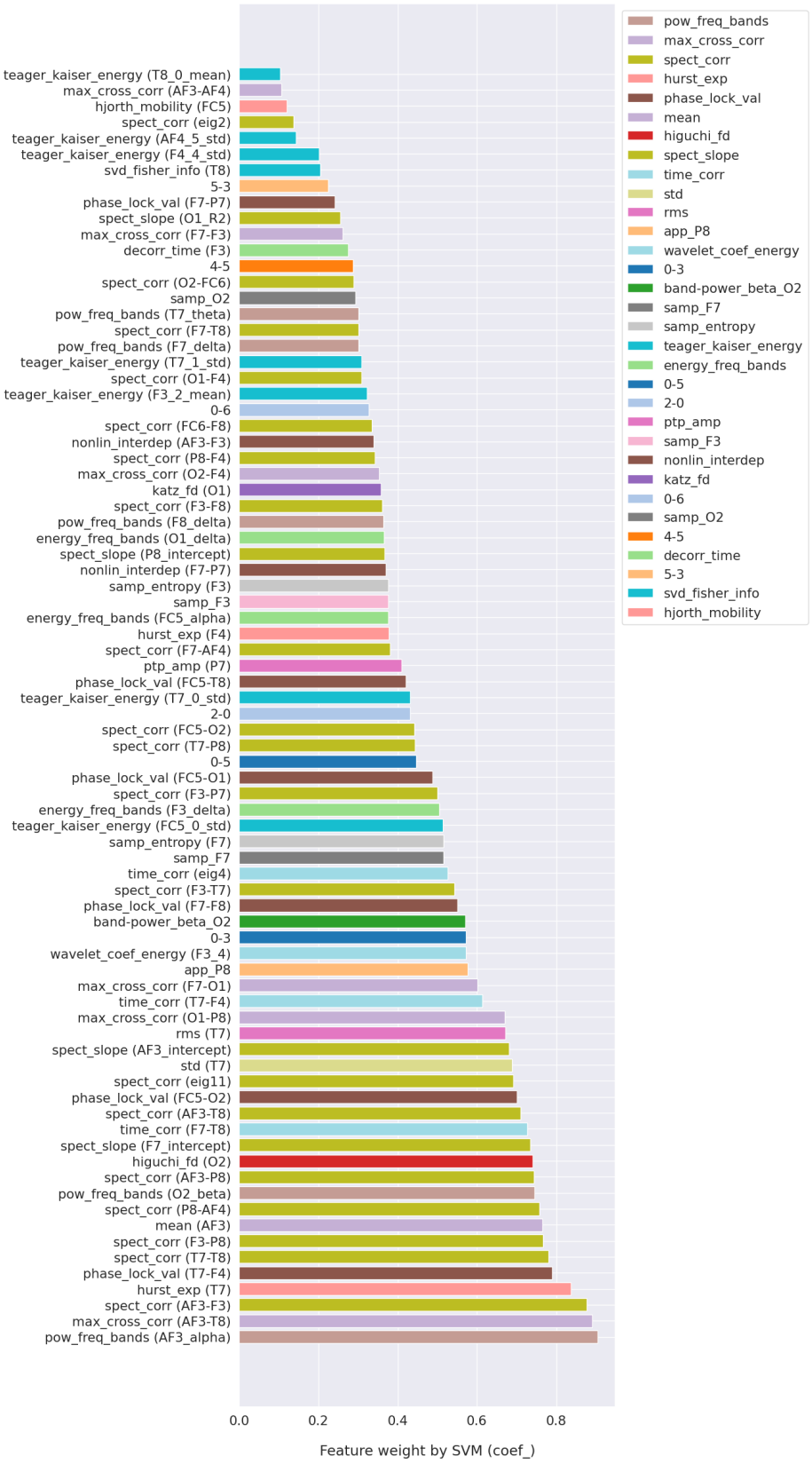

Figure 5.6: Selected features with weights by the SVM model (Moderate vs. Severe). Feature abbreviations are described in Appendix B.

5.1.3 Combined

Previous sections described each phase separately. This section describes the overall performance reached when phases are combined.

The best results for a two-phase combination in four-level classification between Normal, Light, Moderate, and Severe classes were obtained using individual models from previous phases. Overall accuracy reached is 98%, sensitivities of 0.87, 1.00, 0.97, 0.98, and specificities of 1.00, 0.98, 1.00, 0.98, and F1 scores of 0.93, 0.96, 0.97, 0.99 for Normal, Light, Moderate, and Severe class respectively. A confusion matrix is shown in figure 5.7.

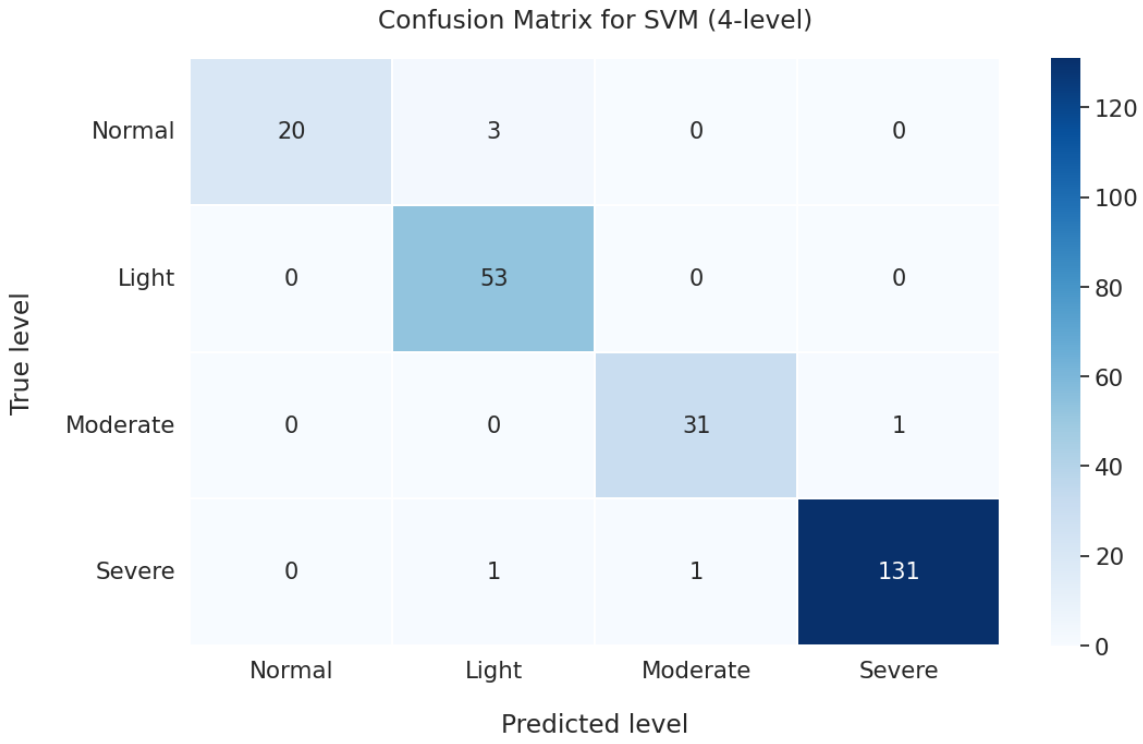

Figure 5.7: Confusion matrix for Moderate and Severe classes.

5.2 Comparative Analysis

The proposed method in this work reached the highest accuracy, sensitivities, specificities, and F1 scores compared with other studies. The proposed method's performance metrics and other studies for two- and four-level classification are shown in table 5.8.

Study	Model	#Features	#Classes	Accuracy (%)	Sensitivity	Specificity	F1 score
Baghdadi et. al [2020]	Stacked Sparse Autoencoder	277	4	86.70	N: 0.85 L: 0.88 M: 0.61 S: 0.95	Not reported	Not reported
Muhammad et. al [2022]	Random Forest	9	2	94.90	N + L: 0.92 M + S: 0.96	Not reported	0.93
		10	4	92.74	N: 0.84 L: 0.91 M: 0.84 S: 0.96	Not reported	0.90
***This work**	Support Vector Machine	100	2	98.00	N + L: 0.95 M + S: 1.00	N + L: 1.00 M + S: 0.95	N + L: 0.97 M + S: 0.99
		102	4	98.00	N: 0.87 L: 1.00 M: 0.97 S: 0.98	N: 1.0 L: 0.98 M: 1.00 S: 0.99	N: 0.93 L: 0.96 M: 0.97 S: 0.99

Figure 5.8: Comparison table of existing results in the literature with results provided in this work. Baghdadi et al. [7], Muhammad et al. [37].

5.3 Discussion

This chapter shows the classification results of the proposed method – classification of two and four anxiety levels. The ground truth is based on the HAM-A questionnaire. For validation of the performance, 10-fold cross-validation was used. It is important to mention that data from one participant are never present in the train and test set simultaneously.

Various methods for feature selection and classification were examined. The best results were achieved using a combination of Ridge Classification with Recursive Feature Elimination for a feature selection and a Support Vector Machine with a linear kernel for classification. A total of 100 and 102 features were selected for two-level and four-level classification, respectively. Because of the imbalances of samples between classes, the model's weights were set to penalize classes with more samples. The results reached an accuracy of 98% for both two-level and four-level. The performance was evaluated on various metrics, such as classification accuracy, sensitivity, specificity, and F1-score.

The proposed method outperformed other existing methods. However, it was shown that more feature types are required to surpass existing methods. In Muhammad et al. [37], only three types of features were used. On the other hand, compared to Baghdadi et al. [7], the proposed method consists of a shorter feature vector.

A combination of features is necessary to achieve high performance, as it was revealed that using a single type of feature does not exceed an accuracy of 70%. The trade-off between a number of features and performance is in favor of performance, as the goal of any medical test is to minimize misdiagnosis, which is the most important thing for the patient. Results presented in this work are within an error rate of 5% in all considered metrics.

The novelty and contribution of this work lie in incorporating microstates as a feature for the classifier, as they were not used before in detecting anxiety. Results demonstrated that no significant results were achieved when using only microstates for classification. However, the performance surpassed existing methods when combining microstates with other time and frequency domain features.

5.4 Directions for Future Research

Quantitative Differences

Exploring the impacts of features from the quantitative perspective can confirm or unveil biomarkers that might account for anxiety. It would be interesting to do a group-level analysis of anxiety levels for selected features; what are the quantitative differences between people having anxiety vs. those who do not? Further, the next step can be to compare the findings with the existing literature.

SAM Prediction

This work used the HAM-A questionnaire as the ground truth for anxiety levels. However, the dataset also includes data from the SAM questionnaire, containing scores for valence and arousal (see appendix A). However, this was out of the scope of this work; thus, I recommend trying classification based on the SAM labels.

Brain Connectivity

Future works can incorporate brain connectivity to identify the causal influences of one neural unit over others within the brain. In addition, brain connectivity is a feature suitable for further interpretation, as it can demonstrate the differences in brain activity from true brain sources. When considering extracting brain connectivity on this dataset, I would put particular focus on data preprocessing, as it was shown that there are still some artifacts left, and connectivity measurements are sensitive to them.

Chapter 6

Conclusion

This work aimed to develop a novel method of anxiety detection from brain signals, in particular electroencephalography (EEG), a non-invasive and cost-effective screening method.

The first chapter was to provide an introduction to the brain, anxiety, and brain imaging techniques. A particular focus here is on the brain parts related to anxiety and the underlying mechanisms. Next, existing diagnostics methods for anxiety are presented, emphasizing the subjective nature of the measurements. Finally, different screening methods for the brain are outlined, with an emphasis on EEG.

The next chapter reviews existing methods of anxiety detection from EEG signals. Subsequently, several existing methods were compared on the DASPS dataset. This dataset consists of EEG recordings of 23 participants, categorized into four anxiety levels: normal, light, moderate, and severe. The dataset is public and was used for this thesis.

The proposed methodology is the most important chapter of this thesis. The scope of the work is presented along with the proposed method, which includes two-level and four-level classification of anxiety levels. Four-level classification uses a two-phase process consisting of multiple binary classifiers. Based on the prediction of the first phase, one of the models in the second phase is selected and predicts the definitive class. The proposed method is based on microstates features, which were not previously utilized for anxiety detection. Microstates were later shown to contribute to the overall performance. Except for microstates, other time and frequency domain features are used and described in this chapter. Implementation details are clarified after the method's proposal, such as used tools, features, feature selection methods, classification models, and hyperparameter tuning.

Finally, the results are presented. Various methods for feature selection and classification were examined. A total of 100 and 102 features were selected for two-level and four-level classification, respectively, by using Ridge regression. The best classification results were obtained using the SVM classifier, reaching an accuracy of 98% for both two-level and four-level. The performance was evaluated on various metrics, such as classification accuracy, sensitivity, specificity, and F1-score. Thesis ends with a discussion and directions for future research.

The proposed method outperformed other existing methods. It was shown that a high number of feature types is required to achieve high performance. Moreover, four-level classification achieves good results using a two-phase process comprising multiple binary models having their own set of features. Despite the positive results, it is essential to continue research on this topic to provide accurate, robust, and explainable diagnostics results, with particular attention to minimizing the chance of misdiagnosis leading to mistreatment, to be able to incorporate such objective methods into medical practice.

Bibliography

[1] Accardo, A., Affinito, M., Carrozzi, M. and Bouquet, F. Use of the fractal dimension for the analysis of electroencephalographic time series. *Biological Cybernetics*. Nov 1997, vol. 77, no. 5, p. 339–350. DOI: 10.1007/s004220050394. ISSN 1432-0770.

[2] Al Ezzi, A., Kamel, N., Faye, I. and Gunaseli, E. Review of EEG, ERP, and brain connectivity estimators as predictive biomarkers of social anxiety disorder. *Front. Psychol.* Frontiers Media SA. may 2020, vol. 11, p. 730.

[3] Al Ezzi, A., Yahya, N., Kamel, N., Faye, I., Alsaih, K. et al. Severity Assessment of Social Anxiety Disorder Using Deep Learning Models on Brain Effective Connectivity. *IEEE Access*. 2021, vol. 9, p. 86899–86913. DOI: 10.1109/ACCESS.2021.3089358.

[4] Ancillon, L., Elgendi, M. and Menon, C. Machine Learning for Anxiety Detection Using Biosignals: A Review. *Diagnostics*. 2022, vol. 12, no. 8. DOI: 10.3390/diagnostics12081794. ISSN 2075-4418.

[5] Arsalan, A. and Majid, M. A study on multi-class anxiety detection using wearable EEG headband. *Journal of Ambient Intelligence and Humanized Computing*. april 2021, vol. 13. DOI: 10.1007/s12652-021-03249-y.

[6] Ashenden, S. *The Era of Artificial Intelligence, Machine Learning, and Data Science in the Pharmaceutical Industry*. Elsevier Science, 2021. ISBN 9780128200452.

[7] Baghdadi, A., Aribi, Y., Fourati, R., Halouani, N., Siarry, P. et al. Psychological stimulation for anxious states detection based on EEG-related features. *Journal of Ambient Intelligence and Humanized Computing*. 2020, vol. 12, no. 8, p. 8519–8533.

[8] Baghdadi, A., Aribi, Y., Fourati, R., Halouani, N., Siarry, P. et al. DASPS: A Database for Anxious States based on a Psychological Stimulation. *CoRR*. 2019, abs/1901.02942. DOI: https://doi.org/10.48550/arXiv.1901.02942.

[9] Bai, Y., Xia, X. and Li, X. A review of resting-state electroencephalography analysis in disorders of consciousness. *Front. Neurol.* Frontiers Media SA. september 2017, vol. 8, p. 471.

[10] Besdata. *Besdata High-Density EEG Caps for Researchers* [online]. [cit. 2022-12-01]. Available at: https://besdatatech.com/high-density-eeg-caps-for-researchers/.

[11] Betts, J. G., Desaix, P., Johnson, E., Johnson, J. E., Korol, O. et al. *Anatomy and Physiology* [online]. 2013 [cit. 2022-11-24]. Available at: http://cnx.org/content/col11496/1.6/.

[12] Biasiucci, A., Franceschiello, B. and Murray, M. M. Electroencephalography. *Current Biology*. 2019, vol. 29, no. 3, p. R80–R85. DOI: https://doi.org/10.1016/j.cub.2018.11.052. ISSN 0960-9822.

[13] Blaus, B. *Multipolar neuron* [online]. 2013 [cit. 2022-12-02]. Available at: https://commons.wikimedia.org/wiki/File:Blausen_0657_MultipolarNeuron.png.

[14] Chatterjee, D., Gavas, R. and Saha, S. K. Detection of mental stress using novel spatio-temporal distribution of brain activations. *Biomedical Signal Processing and Control*. 2023, vol. 82, p. 104526.

[15] Chen, C., Yu, X., Belkacem, A. N., Lu, L., Li, P. et al. EEG-Based Anxious States Classification Using Affective BCI-Based Closed Neurofeedback System. *Journal of Medical and Biological Engineering*. 2021, vol. 41, no. 2, p. 155–164. DOI: 10.1007/s40846-020-00596-7.

[16] Daley, B. *MRI Scanner* [online]. 2016 [cit. 2022-11-24]. Available at: https://4rai.com/images/easyblog_articles/74/3T-MRI.jpg.

[17] Esteller, R., Echauz, J., Tcheng, T., Litt, B. and Pless, B. Line length: An efficient feature for seizure onset detection. In:. February 2001, vol. 2, p. 1707 – 1710 vol.2. DOI: 10.1109/IEMBS.2001.1020545.

[18] Esteller, R., Vachtsevanos, G., Echauz, J. and Litt, B. A Comparison of waveform fractal dimension algorithms. *Circuits and Systems I: Fundamental Theory and Applications, IEEE Transactions on*. march 2001, vol. 48, p. 177 – 183. DOI: 10.1109/81.904882.

[19] Gupta, D., Shariat, M. H., Baetz Dougan, M., Hashemi, J., Akl, S. et al. Novel Automated Paced Fractionation Detection Algorithm for Ablating Ventricular Tachycardia. *Journal of Biomedical Science and Engineering*. january 2016, vol. 09, p. 488–500. DOI: 10.4236/jbise.2016.910044.

[20] Haller, M., Donoghue, T., Peterson, E., Varma, P., Sebastian, P. et al. Parameterizing neural power spectra. *BioRxiv*. Cold Spring Harbor Laboratory. 2018. DOI: 10.1101/299859.

[21] Hassanin, O., Al Shargie, F., Tariq, U. and Al Nashash, H. Asymmetry of Regional Phase Synchrony Cortical Networks Under Cognitive Alertness and Vigilance Decrement States. *IEEE Transactions on Neural Systems and Rehabilitation Engineering*. 2021, vol. 29, p. 2378–2387. DOI: 10.1109/TNSRE.2021.3125420.

[22] Hastie, T., Tibshirani, R. and Friedman, J. *The elements of statistical learning: data mining, inference and prediction*. 2nd ed. Springer, 2009.

[23] Hernandez Valle, F. *Pulsed-electromagnet EMAT for high temperature applications*. September 2011.

[24] Hjorth, B. EEG analysis based on time domain properties. *Electroencephalography and Clinical Neurophysiology*. 1970, vol. 29, no. 3, p. 306–310. DOI: https://doi.org/10.1016/0013-4694(70)90143-4. ISSN 0013-4694.

[25] Hoffmann, F., Köppen, M., Klawonn, F. and Roy, R. *Soft Computing: Methodologies and Applications*. Springer, 2005. Advances in Intelligent and Soft Computing. ISBN 9783540257264.

[26] Hosák, L. and Hrdlička, M. *Psychiatry and pedopsychiatry*. 1st ed. Charles University, Karolinum Press, 2016. ISBN 978-80-246-3378-7.

[27] Jirsa, V. and Müller, V. Cross-frequency coupling in real and virtual brain networks. *Front. Comput. Neurosci.* Frontiers Media SA. july 2013, vol. 7, p. 78.

[28] Kaan, E. Event-Related Potentials and Language Processing: A Brief Overview. *Lang. Linguistics Compass*. 2007, vol. 1, p. 571–591.

[29] Kamel, N. and Malik, A. S. *EEG/ERP Analysis: Methods and Applications*. 1st ed. CRC Press, 2014 [cit. 2022-12-24]. ISBN 978-1482224696.

[30] Kehtarnavaz, N. *Digital Signal Processing System Design, Second Edition: LabVIEW-Based Hybrid Programming*. 2ndth ed. USA: Academic Press, Inc., 2008. ISBN 0123744903.

[31] Kill, J. B., Ciarelli, P. M. and Côco, K. F. Analysis of EEG microstates to predict epileptic seizures in an online approach. *Research on Biomedical Engineering*. 2022, vol. 38, no. 2, p. 409–421. DOI: 10.1007/s42600-021-00197-6.

[32] Luck, S. *An Introduction to the Event-Related Potential Technique, second edition*. MIT Press, 2014. A Bradford Book. ISBN 9780262525855.

[33] Luu, P., Flaisch, T. and Tucker, D. M. Medial Frontal Cortex in Action Monitoring. *Journal of Neuroscience*. Society for Neuroscience. 2000, vol. 20, no. 1, p. 464–469. DOI: 10.1523/JNEUROSCI.20-01-00464.2000. ISSN 0270-6474.

[34] Michael, J. A., Wang, M., Kaur, M., Fitzgerald, P. B., Fitzgibbon, B. M. et al. EEG correlates of attentional control in anxiety disorders: A systematic review of error-related negativity and correct-response negativity findings. *Journal of Affective Disorders*. 2021, vol. 291, p. 140–153. DOI: https://doi.org/10.1016/j.jad.2021.04.049. ISSN 0165-0327.

[35] Michel, C. M. and Koenig, T. EEG microstates as a tool for studying the temporal dynamics of whole-brain neuronal networks: A review. *NeuroImage*. 2018, vol. 180, p. 577–593. DOI: https://doi.org/10.1016/j.neuroimage.2017.11.062. Brain Connectivity Dynamics.

[36] Mormann, F., Andrzejak, R. G., Elger, C. E. and Lehnertz, K. Seizure prediction: the long and winding road. *Brain*. september 2006, vol. 130, no. 2, p. 314–333. DOI: 10.1093/brain/awl241. ISSN 0006-8950.

[37] Muhammad, F. and Al Ahmadi, S. Human state anxiety classification framework using EEG signals in response to exposure therapy. *PLoS One*. Public Library of Science (PLoS). march 2022, vol. 17, no. 3.

[38] Omar, B. *Biology final exam workbook* [online]. 2021 [cit. 2022-11-24]. Available at: https://sites.google.com/view/biologyerettsegi?pli=1.

[39] Pantazis, D. and Adler, A. MEG Source Localization via Deep Learning. *Sensors*. june 2021, vol. 21, p. 4278. DOI: 10.3390/s21134278.

[40] Poppelaars, E., Klackl, J., Pletzer, B. and Jonas, E. Delta-beta cross-frequency coupling as an index of stress regulation during social-evaluative threat. *Biological Psychology*. february 2021, vol. 160, p. 108043. DOI: 10.1016/j.biopsycho.2021.108043.

[41] Richman, J. S. and Moorman, J. R. Physiological time-series analysis using approximate entropy and sample entropy. *American Journal of Physiology-Heart and Circulatory Physiology*. 2000, vol. 278, no. 6, p. H2039–H2049. DOI: 10.1152/ajpheart.2000.278.6.H2039. PMID: 10843903.

[42] Roberts, S. J., Penny, W. and Rezek, I. Temporal and spatial complexity measures for electroencephalogram based brain-computer interfacing. *Medical & Biological Engineering & Computing*. Jan 1999, vol. 37, no. 1, p. 93–98. DOI: 10.1007/BF02513272.

[43] Rossion, B., Joyce, C. A., Cottrell, G. W. and Tarr, M. J. Early lateralization and orientation tuning for face, word, and object processing in the visual cortex. *NeuroImage*. 2003, vol. 20, no. 3, p. 1609–1624. DOI: https://doi.org/10.1016/j.neuroimage.2003.07.010. ISSN 1053-8119.

[44] Russell, S. and Norvig, P. *Artificial Intelligence: A Modern Approach*. 3rd ed. Prentice Hall, 2010.

[45] Stam, C. J., Nolte, G. and Daffertshofer, A. Phase lag index: Assessment of functional connectivity from multi channel EEG and MEG with diminished bias from common sources. *Human Brain Mapping*. 2007, vol. 28, no. 11, p. 1178–1193. DOI: https://doi.org/10.1002/hbm.20346.

[46] Standring, S. *Gray's Anatomy: The Anatomical Basis of Clinical Practice*. 41th ed. Elsevier Limited, 2016. ISBN 978-0-7020-5230-9.

[47] Strathmann, H., Lakshminarayanan, B., Ialongo, A., Bohner, G., Huh, B. D. et al. Seizure Detection Challenge The Fitzgerald team solution. In:. 2015.

[48] Subasi, A. *Practical Machine Learning for Data Analysis Using Python*. June 2020. ISBN 9780128213797.

[49] Tadel, F., Baillet, S., Mosher, J. C., Pantazis, D. and Leahy, R. M. Brainstorm: a user-friendly application for MEG/EEG analysis. *Comput. Intell. Neurosci.* Hindawi Limited. april 2011, vol. 2011, p. 879716.

[50] Teixeira, C., Direito, B., Feldwisch Drentrup, H., Valderrama, M., Costa, R. et al. EPILAB: A software package for studies on the prediction of epileptic seizures. *Journal of Neuroscience Methods*. 2011, vol. 200, no. 2, p. 257–271. DOI: https://doi.org/10.1016/j.jneumeth.2011.07.002.

[51] Xie, Y., Yang, B., Lu, X., Zheng, M., Fan, C. et al. Anxiety and depression diagnosis method based on brain networks and convolutional neural networks. *Annu. Int. Conf. IEEE Eng. Med. Biol. Soc.* july 2020, vol. 2020, p. 1503–1506.

[52] Yu, S., Zheng, N., Ma, Y., Wu, H. and Chen, B. A Novel Brain Decoding Method: A Correlation Network Framework for Revealing Brain Connections. *IEEE Transactions on Cognitive and Developmental Systems*. 2019, vol. 11, no. 1, p. 95–106. DOI: 10.1109/TCDS.2018.2854274.

[53] Zhuang, N., Zeng, Y., Tong, L., Zhang, C., Zhang, H. et al. Emotion Recognition from EEG Signals Using Multidimensional Information in EMD Domain. *BioMed Research International*. Hindawi. Aug 2017, vol. 2017. DOI: 10.1155/2017/8317357. ISSN 2314-6133.

Appendix A

Anxiety Questionnaires

HAM-A

Hamilton Anxiety Rating Scale (HAM-A)

Below is a list of phrases that describe certain feeling that people have. Rate the patients by finding the answer which best describes the extent to which he/she has these conditions. Select one of the five responses for each of the fourteen questions.

0 = Not present, 1 = Mild, 2 = Moderate, 3 = Severe, 4 = Very severe.

1 Anxious mood [0] [1] [2] [3] [4]

Worries, anticipation of the worst, fearful anticipation, irritability.

2 Tension [0] [1] [2] [3] [4]

Feelings of tension, fatigability, startle response, moved to tears easily, trembling, feelings of restlessness, inability to relax.

3 Fears [0] [1] [2] [3] [4]

Of dark, of strangers, of being left alone, of animals, of traffic, of crowds.

4 Insomnia [0] [1] [2] [3] [4]

Difficulty in falling asleep, broken sleep, unsatisfying sleep and fatigue on waking, dreams, nightmares, night terrors.

5 Intellectual [0] [1] [2] [3] [4]

Difficulty in concentration, poor memory.

6 Depressed mood [0] [1] [2] [3] [4]

Loss of interest, lack of pleasure in hobbies, depression, early waking, diurnal swing.

7 Somatic (muscular) [0] [1] [2] [3] [4]

Pains and aches, twitching, stiffness, myoclonic jerks, grinding of teeth, unsteady voice, increased muscular tone.

8 Somatic (sensory) [0] [1] [2] [3] [4]

Tinnitus, blurring of vision, hot and cold flushes, feelings of weakness, pricking sensation.

9 Cardiovascular symptoms [0] [1] [2] [3] [4]

Tachycardia, palpitations, pain in chest, throbbing of vessels, fainting feelings, missing beat.

10 Respiratory symptoms [0] [1] [2] [3] [4]

Pressure or constriction in chest, choking feelings, sighing, dyspnea.

11 Gastrointestinal symptoms [0] [1] [2] [3] [4]

Difficulty in swallowing, wind abdominal pain, burning sensations, abdominal fullness, nausea, vomiting, borborygmi, looseness of bowels, loss of weight, constipation.

12 Genitourinary symptoms [0] [1] [2] [3] [4]

Frequency of micturition, urgency of micturition, amenorrhea, menorrhagia, development of frigidity, premature ejaculation, loss of libido, impotence.

13 Autonomic symptoms [0] [1] [2] [3] [4]

Dry mouth, flushing, pallor, tendency to sweat, giddiness, tension headache, raising of hair.

14 Behavior at interview [0] [1] [2] [3] [4]

Fidgeting, restlessness or pacing, tremor of hands, furrowed brow, strained face, sighing or rapid respiration, facial pallor, swallowing, etc.

Figure A.1: Hamilton Anxiety Rating Scale (HAM-A).

SAM

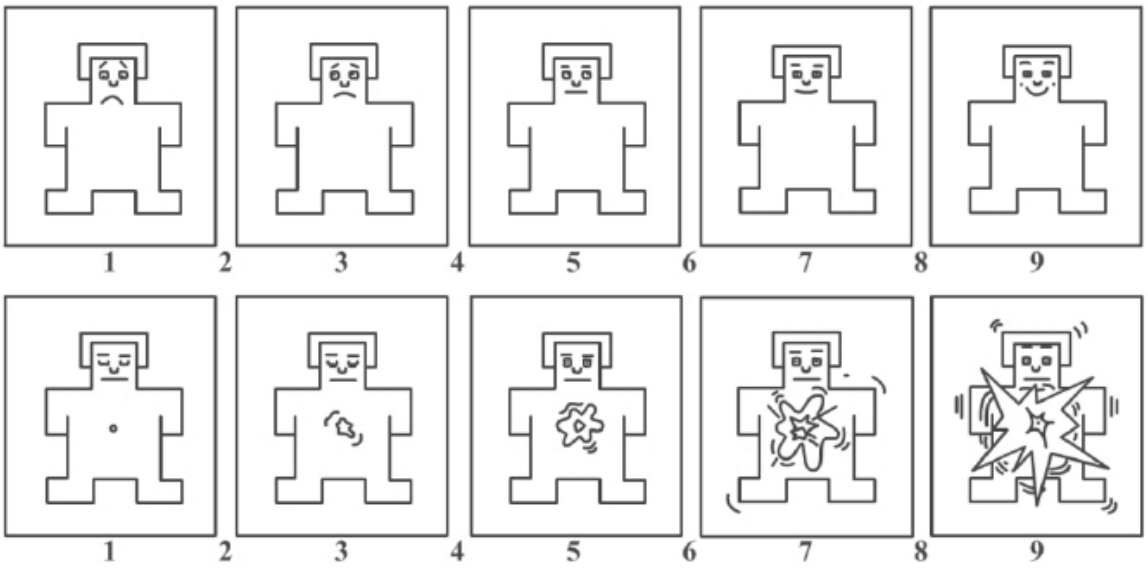

Figure A.2: Self assessment manikin (SAM). First row represents Valence scale, ranging from negative to positive. Second row represents Arousal scale, ranging from calm to excited.

Appendix B

Feature Abbreviations

Features names in plot are shown in format `"<feature-name> (<feature-details>)"`, where `<feature-details>` indicates either channel, pair of channels, or any other descriptor provided by the MNE-Features[1] package. The list of feature abbreviations with their corresponding description:

- `0-1` - transition probability from microstate 0 to microstate 1
- `0-3` - transition probability from microstate 0 to microstate 3
- `0-5` - transition probability from microstate 0 to microstate 5
- `0-6` - transition probability from microstate 0 to microstate 6
- `0_occurence` - occurence of microstate 0
- `2-0` - transition probability from microstate 2 to microstate 0
- `4-5` - transition probability from microstate 4 to microstate 5
- `4-6` - transition probability from microstate 4 to microstate 6
- `5-0` - transition probability from microstate 5 to microstate 0
- `5-3` - transition probability from microstate 5 to microstate 3
- `app_P8` - approximate entropy of P8 channel
- `asymmetry_index_FC5-FC6_8-12` - AI of FC5-FC6 channels in alpha band
- `band-power_alpha_T8` - alpha band power of T8 channel
- `band-power_beta_O2` - beta band power of O2 channel
- `band-power_delta_F7` - delta band power of F7 channel
- `band-power_delta_O2` - delta band power of O2 channel
- `band-power_delta_P8` - delta band power of P8 channel
- `band-power_theta_F7` - theta band power of F7 channel

[1] https://mne.tools/mne-features

- `band-power_theta_FC6` - theta band power of FC6 channel
- `decorr_time` - decorrelation time
- `energy_freq_bands` - energy in frequency bands
- `higuchi_fd` - Higuchi fractal dimension
- `hjorth_complexity_spect` - Hjorth complexity of spectrum
- `hjorth_complexity` - Hjorth complexity
- `hjorth_mobility` - Hjorth mobility
- `hurst_exp` - Hurst exponent
- `katz_fd` - Katz fractal dimension
- `kurtosis` - kurtosis
- `line_length` - line length
- `max_cross_corr` - maximum cross correlation
- `mean` - mean
- `nonlin_interdep` - nonlinear interdependence
- `phase_lock_val` - phase locking value
- `pow_freq_bands` - power in frequency bands
- `ptp_amp` - peak-to-peak amplitude
- `quantile` - quantile
- `rms` - root mean square
- `samp_F3` - sample entropy of F3 channel
- `samp_F7` - sample entropy of F7 channel
- `samp_O2` - sample entropy of O2 channel
- `samp_entropy` - sample entropy
- `spect_corr` - spectral correlation
- `spect_edge_freq` - spectral edge frequency
- `spect_slope` - spectral slope
- `std` - standard deviation
- `svd_entropy` - singular value decomposition entropy
- `svd_fisher_info` - singular value decomposition Fisher information

- `teager_kaiser_energy` - Teager-Kaiser energy
- `time_corr` - time correlation
- `wavelet_coef_energy` - wavelet coefficient energy
- `zero_crossings` - zero crossings

Appendix C

Contents of SD card

thesis/ text of the thesis in PDF and source code in LaTeX

dataset/ DASPS dataset, preprocessed data

features/ calculated features

models/ trained models

sources/ source codes, jupyter notebooks

README.md user manual